NASA Contractor Report 178215

ICASE REPORT NO. 86-83

ICASE

THE NONLINEAR DEVELOPMENT OF GORTLER VORTICES IN GROWING BOUNDARY LAYERS

Philip Hall

(NASA-CR-178215) THE NONLINEAR DEVELOPMENT OF GORTLER VORTICES IN GROWING BOUNDARY LAYERS Final Report (NASA) 53 p CSCL 20D

N87-16245

Unclas

G3/34 43307

Contract No. NAS1-18107

December 1986

INSTITUTE FOR COMPUTER APPLICATIONS IN SCIENCE AND ENGINEERING
NASA Langley Research Center, Hampton, Virginia 23665

Operated by the Universities Space Research Association

National Aeronautics and Space Administration

Langley Research Center
Hampton, Virginia 23665

THE NONLINEAR DEVELOPMENT OF GORTLER VORTICES IN GROWING BOUNDARY LAYERS

Philip Hall
Department of Mathematics
Exeter University

ABSTRACT

The development of Gortler vortices in boundary layers over curved walls in the nonlinear regime is investigated. The growth of the boundary layer makes a parallel flow analysis impossible except in the high wavenumber regime so in general the instability equations must be integrated numerically. Here the spanwise dependence of the basic flow is described using a Fourier series expansion whilst the normal and streamwise variations are taken into account using finite differences. The calculations suggest that a given disturbance imposed at some position along the wall will eventually reach a local equilibrium state essentially independent of the initial conditions. In fact, the equilibrium state reached is qualitatively similar to the large amplitude high wave-number solution described asymptotically by Hall (1982b). In general, it is found that the nonlinear interactions are dominated by a ´mean field´ type of interaction between the mean flow and the fundamental. Thus, even though higher harmonics of the fundamental are necessarily generated, most of the disturbance energy is confined to the mean flow correction and the fundamental. A major result of our calculations is the finding that the downstream velocity field develops a strongly inflectional character as the flow moves downstream. The latter result suggests that the major effect of Gortler vortices on boundary layers of practical importance might be to make them highly receptive to rapidly growing Rayleigh modes of instability.

This work was supported under the National Aeronautics and Space Administration under NASA Contract No. NAS1-18107 while the author was in residence at the Institue for Computer Applications in Science and Engineering (ICASE), NASA Langley Research Center, Hampton, VA 23665.

INTRODUCTION

Our concern is with the effect of nonlinearity on the growth of Taylor-Gortler vortices in developing boundary layers. The presence of such vortices in many flows of practical importance such as those which occur over turbine blades or over laminar flow aerofoils has recently stimulated much research aimed at understanding their structure in the linear regime. However the nonlinear problem has, apart from the high wavenumber analysis of Hall (1982b), received little attention because of the difficulty in taking care of non-parallel effect. At high wavenumbers Hall found that nonlinear effects have a stabilizing effect and prevent the exponential growth of the vortices predicted by linear theory.

In previous investigations Hall (1982a, 1983), hereafter referred to as I, II respectively, looked at the linear Gortler problem and showed that except at high wavenumbers parallel flow calculations for the Gortler problem are not valid because the streamwise and normal dependences of the vortices cannot be separated. In fact, in the only regime where the instability equations can be reduced to ordinary differential equations, the asymptotic theory of I provides trivially a neutral curve or growth rate at least as accurate as that produced by the parallel flow theories. Here by 'parallel' we simply mean any theory which ignores any term in the linear instability equations. Of course the parallel flow theories correspond to truncations of the instability equations of varying severity. Thus for example Gortler (1940), (later corrected numerically by Hammerlin (1956)), retained only the terms which would be present in the corresponding Taylor-Couette flow calculation whilst Smith (1955) retained many terms associated with the growth of the boundary layer. Other truncations of the instability equations have been given by, for example, Floryan and Saric (1978) and Herbert (1976).

At O(1) wavenumbers the various parallel flow theories give quite different results and in the most extreme cases predict instability at zero Gortler number or zero wavenumber. In II it was argued that at O(1) wavenumbers these calculations are necessarily incorrect because their neglect of streamwise derivatives of the disturbance velocity field gives the wrong structure for the disturbance at the edge of the boundary layer. If these terms are retained it was shown that the vortices decay to zero at the edge of the boundary layer at a rate independent of the vortex wavenumber. In fact the linear instability equations are parabolic in the streamwise direction and can therefore be solved numerically by marching downstream from some initial location. A 'local' neutral position can then be defined to be the point where some disturbance flow quantity has a zero rate of change along the wall. This position depends on the location and form for the initial disturbance so that the notion of a unique neutral curve is not tenable for the Gortler problem. However, at high wavenumbers the numerical calculations of II converged to the unique asymptotic result of I.

Here we shall extend the parallel flow calculations of I to the nonlinear regime appropriate to disturbances with wavenumber of O(1). At higher wavenumbers the asymptotic high wavenumber theory of Hall (1982b), hereafter referred to as III, showed that in this regime the nonlinear problem is dominated by a 'mean field' type of interaction rather than one typical of a Stuart-Watson approach. It was shown in III that the mean flow correction driven by a finite amplitude vortex ultimately becomes larger than the vortices driving it. At sufficiently large amplitude the mean flow correction described in III would cause the basic state to develop an inflection point and therefore possibly make the boundary layer susceptible to rapidly growing Rayleigh instabilities. A primary aim of the calculation is to confirm the latter result at large wavenumbers and investigate the situation at O(1) wavenumbers. Our calculations will also enable linear instability calculations of finite amplitude Gortler vortices to be ultimately carried out along the lines of the recent calculation of Bennett and Hall (1986). The latter authors were concerned with the corresponding internal fully developed flow between concentric cylinders and showed that even small amplitude vortices cause a massive destabilization of the undisturbed flow to Tollmien-Schlichting waves.

Since there is no rational way to reduce the nonlinear nonparallel Gortler problem to a series of ordinary differential equations using the Stuart-Watson method we solve the equations governing finite amplitude vortices using a numerical method based on the finite difference formulation of II together with a Fourier expansion to take care of the spanwise dependence of the flow. The vortices are assumed to be steady so that the equations governing their development can be marched downstream from the initial location where the disturbance is imposed. This is done using the implicit scheme of II together with an iteration procedure to take care of the nonlinear terms which are now present in the calculation. At each downstream location the energy in each Fourier mode can be calculated in order to monitor the development of the instability. We shall see that nonlinear effects prevent the exponential growth of the disturbances predicted by linear theory so that, at least in the limited number of cases we have investigated, nonlinear effects are stabilizing. We shall also see that any given vortex will sufficiently far downstream develop a structure consistent with the nonlinear theory of III. The latter result is not surprising since the effective vortex wavenumber increases in the streamwise direction until the asymptotic theory of III applies.

Apart from the arbitrariness associated with the linear problem described in II the nonlinear problem introduces further complications because of the further freedom we now have when imposing the initial disturbance. Our calculations are, of course, restricted to a finite number of situations but nevertheless the similarity between the results enables us to make some tentative conclusions about the role of nonlinear effects in the Gortler problem. The procedure adopted in the rest of the paper is as follows: in Section 2 we formulate the nonlinear instability equations and describe a numerical scheme which can be used to integrate them. In section 3 we describe the results we have obtained and use them to draw some conclusions about non-linear Gortler vortices.

2. FORMULATION OF THE INSTABILITY EQUATIONS AND THEIR SOLUTION.

Consider the flow of a viscous fluid of kinematic viscosity ν over a wall of curvature $a^{-1}\kappa(x/\ell)$. Here ℓ and a are typical length scales associated with the downstream development of the flow and the local radius of curvature of the wall. We take U_0 to be a typical flow speed and define a Reynolds number Re by

$$Re = \frac{U_0 \ell}{\nu} , \tag{2.1}$$

and consider the limit of $Re \to \infty$ with the Gortler number G, defined by

$$G = \frac{2\ell}{a} Re^{\frac{1}{2}} , \tag{2.2}$$

held fixed. Let us take (X,Y,Z) to be dimensionless variables in the streamwise, normal and spanwise directions scaled on ℓ, $Re^{\frac{1}{2}}\ell$, $Re^{\frac{1}{2}}\ell$ respectively. The velocity field is taken to be of the form

$$\bar{u} = U_0(\bar{u}(X,Y) + U(X,Y,Z), \ Re^{-\frac{1}{2}}(\bar{v}(X,Y) + V(X,Y,Z)), \ Re^{-\frac{1}{2}}W(X,Y,Z)) , \tag{2.3}$$

where $(\bar{u}(X,Y), \bar{v}(X,Y))$ corresponds to a Blasius boundary layer and (U,V,W) and the corresponding pressure perturbation P are functions of X,Y,Z. Following the procedure outlined in III it is an easy matter to show from the Navier-Stokes equations that, correct to order $Re^{-\frac{1}{2}}$, U,V,W,P satisfy

$$U_X + V_Y + W_Z = 0 ,$$

$$U_{YY} + U_{ZZ} - V\bar{u}_Y = \bar{u}U_X + U\bar{u}_X + V\bar{u}_Y + \bar{v}U_Y + Q_1 ,$$

$$V_{YY} + V_{ZZ} - G\kappa\bar{u}U - P_Y = \bar{u}V_X + U\bar{v}_X + \bar{v}V_Y + V\bar{v}_Y + Q_2 ,$$

$$W_{YY} + W_{ZZ} - P_Z = \bar{u}W_X + \bar{v}W_Y + Q_3 , \qquad (2.4a,b,c)$$

where Q_1, Q_2, Q_3 are defined by

$$Q_1 = UU_X + VU_Y + WU_Z ,$$

$$Q_2 = UV_X + VV_Y + WV_Z + \tfrac{1}{2}G\kappa U^2 ,$$

$$Q_3 = UW_X + VW_Y + WW_Z . \qquad (2.5a,b,c)$$

If the nonlinear functions Q_1, Q_2, Q_3 are set equal to zero in the above equations we recover the equations of II. The nonlinear theory of III gives an asymptotic solution of (2.4) valid in the limit of $\frac{\partial}{\partial z} >> 1$. This limit is more relevant than it might appear to be at first sight since it corresponds to the large X state of any initial disturbance imposed on the flow. Thus in our numerical calculations we expect to recover qualitatively the results of III sufficiently far downstream from where the critical disturbance is introduced.

In order to reduce (2.4) to a form more suitable for computational purposes we can eliminate P and W from the linear terms in (2.4c,d) to give

$$V\{\bar{u}_{XYY} + \frac{\partial^4}{\partial Z^4} - \bar{v}_Y \frac{\partial}{\partial Z^2}\} + \bar{v}_X U_{YY} + \{\bar{u}_{XYY} - \bar{v}_X \frac{\partial^2}{\partial Z^2} - \kappa G\bar{u} \frac{\partial^2}{\partial Z^2}\} U$$

$$+ \{\bar{u}_{YY} - \bar{u} \frac{\partial^2}{\partial Y^2} - \bar{u} \frac{\partial^2}{\partial Z^2}\} V_X + 2\{\bar{u}_{XY} + \bar{u}_X \frac{\partial}{\partial Y}\} U_X$$

$$+ V_{YYYY} - \bar{v}V_{YYY} - \{\bar{v}_Y - 2 \frac{\partial^2}{\partial Z^2}\} V_{YY} + \{\bar{u}_{XY} - \bar{v} \frac{\partial^2}{\partial Z^2}\} V_Y$$

$$= Q_{1XY} + Q_{2ZZ} - Q_{3YZ} \qquad (2.6)$$

where Q_1, Q_2 and Q_3 are given by (2.5a,b,c) respectively.

Suppose that U, V and W are then expanded in the form

$$U = U_0 + \sum_{n=1}^{\infty} U_n(X,Y) \cos naZ ,$$

$$V = V_0 + \sum_{n=1}^{\infty} V_n(X,Y) \cos naZ$$

$$W = \sum_{n=1}^{\infty} W_n(X,Y) \sin naZ \qquad (2.7a,b,c)$$

where we have anticipated the well-known result that the nonlinear interactions which occur in the Taylor-Gortler problem do not generate a mean flow in the spanwise direction. We then substitute for (U,V,W) from (2.7) into (2.4a) and (2.6) and equate like Fourier coefficients. This procedure shows that the mean flow correction satisfies

$$U_{0YY} - V_0\bar{u}_Y - \bar{u}U_{0X} - U_0\bar{u}_X - \bar{v}U_{0Y} = U_0U_{0X} + V_0U_{0Y} + F_0 \qquad (2.8)$$

where $F_0 = +\frac{1}{2} \sum_{m=1}^{\infty} \{V_m U_{mY} - U_m V_{mY} - 2maU_m W_m\}$,

and V_0 is determined by

$$\frac{\partial U_0}{\partial X} + \frac{\partial V_0}{\partial Y} = 0 \quad . \qquad (2.9)$$

For computational purposes we must of course truncate the infinite sums in (2.7) at some suitably large value for the upper limit. We therefore replace the upper limit in (2.7) by N .

Similarly we find that U_n satisfies

$$U_{nYY} - a^2U_n - \bar{\bar{u}}U_{nX} - U_n\bar{\bar{u}}_X - V_n\bar{\bar{u}}_Y - \bar{\bar{v}}U_{nY}$$

$$= F_n = \sum_{\substack{m=1\\ N\neq 1}}^{N-1} V_{n-m} U_{mY} - U_{n-m} V_{mY} + maW_{n-m} U_m - ma\, U_{n-m}W_m$$

$$+ \sum_{\substack{m=1\\ n\neq N}}^{N-n} V_{n+m} U_{mY} - U_{n+m} V_{mY} - ma\, U_mW_{n+m} - ma\, U_{n+m} W_m$$

$$+ \sum_{\substack{m = n+1\\ n\neq 1}}^{N} V_{m-n} U_{mY} - U_{m-n} V_{mY} - ma\, W_{m-n} U_m - ma\, U_{m-n} W_m \qquad (2.10)$$

where $\bar{\bar{u}} = \bar{u} + U_0$ and $\bar{\bar{v}} = \bar{v} + V_0$.

An equation of the same form can be derived from (2.6) by equating to zero the coefficient of $\cos naz$. Suppose that U_0, V_0, U_n, V_n, W_n, for $n = 1,2,3.....$ are known at X , we now describe how (2.8) and (2.10) can be stepped forward to $X + \varepsilon$. The scheme used is essentially that described in II together with an iteration procedure to take care of the nonlinear terms now present. Thus for example the mean flow equation (2.8) is discretized using finite differences in the X and Y directions to give

$$\frac{U_0^{n+1\ m+1} - 2U_0^{n\ m+1} + U_0^{n-1\ m+1}}{h^2} \frac{-\bar{u}^{nm}}{\varepsilon}\left\{U_0^{n\ m+1} - U_0^{n\ m}\right\} - \bar{v}^{nm}\left\{\frac{V_0^{n+1\ m} \quad V_0^{n-1\ m}}{2h}\right\}$$

$$- U_0^{nm}\,\bar{u}_X^{nm} - V_0^{nm}\bar{u}_Y^{nm} = \frac{U_0^{nk+1}}{\varepsilon}\left\{U_0^{nk+1} - U_0^{nk}\right\} + V_0^{nk+1}\left\{\frac{U_0^{n+1\ k+1} - U_0^{n-1\ kn}}{2h}\right\} + F_0^{nk+1}$$

(2.11)

Here indices n, m refer to the grid point $X = X_0 + m$, $Y = nh$.

The nonlinear terms on the right hand side of (2.11) are initially evaluated with $k = m-1$ and the resulting tridiagonal system can be solved to give U_0 at $X = X_0 + (m + 1)\varepsilon$. The equation (2.10) can be stepped forward in a similar manner to give U_m, $m = 1, .., N$ at $X = X_0 + (m + 1)\varepsilon$. Likewise the V equation can be stepped forward by solving a pentadiagonal system. At this stage the nonlinear terms can be expressed in terms of the velocity field now calculated at $X = X_0 + (m + 1)\varepsilon$. The equation can then be solved again for the flow quantities at $X = X_0 + (m + 1)\varepsilon$ and the iteration procedure continued until the change in $U_0^{m+1\ n}$, $U_1^{m+1\ m}$ etc is sufficiently small. Thus (2.11) and the corresponding equations for U_m, V_m are effectively solved with $k = m$ by iterating on the nonlinear terms on the right hand side.

3. RESULTS AND DISCUSSION

We shall firstly describe some results obtained in order to verify the numerical scheme used. These calculations were carried out at various values of the parameters of the problem but here we shall concentrate on the case

$$a = .2, \quad G = .0288, \quad \kappa(X) = \frac{X}{20} \quad . \tag{3.1}$$

This choice for the curvature function κ means that the effective local Gortler number varies like $X^{5/2}$ whilst the local wavenumber varies like $X^{\frac{1}{2}}$. The asymptotic theory of I showed that the neutral curve which can be uniquely defined at high wavenumbers has the Gortler number proportional to the fourth power of the wavenumber and therefore (3.1) corresponds to a disturbance which remains in the unstable region when X increases.

The basic state was disturbed at $X = 55.$ by imposing the condition

$$U_1(\eta) = \eta^6 e^{-\eta^2} \quad , \quad V_1(\eta) = 0 \tag{3.2}$$

and integrating the linearized equations to $X = 100$. At this stage the disturbance is almost locally neutral stable according to the criterion of II and the linear velocity field was given an amplitude Δ equal to the maximum X-disturbance velocity component. The nonlinear equations were then integrated for $X > 100$ and the local growth rates and energies of the different harmonics were calculated. We defined the energy of the nth harmonic to be

$$E_n = \int_0^1 \{U_n^2(X,Y) + V_n^2(X,Y) + W_n^2(X,Y)\}dY, \quad n = 1,2,... \tag{3.3}$$

and the energy of the mean flow distortion was defined by

$$E_o = \int_0^1 \{U_0^2(X,Y)\}dY. \tag{3.4}$$

Here we have omitted the contribution from V_o since $V_0 \to$ constant when $Y \to \infty$. The growth rate $\theta_n(X)$ of the nth mode was defined by

$$\theta_n(X) = \frac{dE_n}{dX} E_n^{-1} \tag{3.5}$$

so that for a parallel boundary layer in the linear regime σ_n would be twice the linear spatial amplification rate.

We know from the nonparallel calculations of I that $\theta_1(x)$ initially depends sensitively on the form and location of the initial disturbance. Here the situation is more complex because we can specify each Fourier mode and the mean flow distribution. In Figure 1 we have shown the dependence of θ_1, $c \geqslant 1$ on X for five different values of Δ the disturbance flow amplitude. Apart from the fundamental all the Fourier components of the disturbance were set equal to zero at the initial location. The calculations shown were carried out with $N = 4$, $\epsilon = .025$, $y_\infty = 150$. Similar calculations were carried out by changing N to 8, ϵ to .05 and y_∞ to 100 in turn. The results agreed with those of Figure 1 to the graphical accuracy of that Figure.

We see in Figure 1 that for a 0.5% disturbance the growth rate over the interval shown is indistinguishable from linear theory. At higher values of Δ the growth rate is initially increased above the linear value and then falls below it when X increases. The amount by which the growth rate is decreased from the linear value increases with Δ and we conclude that in this situation nonlinear effects are stabilizing. We attribute the initial increase in the growth rate to the relatively quick change in flow structure which must necessarily occur when nonlinear effects are operational.

In Figure 2 we have shown the corresponding growth rates for the first harmonic, again we see that after the initial period of growth the disturbance growth decreases with . We note that the growth rates of Figures 1, 2 are comparable even though the first harmonic is locally neutrally stable at a higher Gortler Number than is the fundamental. This growth of the first harmonic is of course driven by nonlinear effects. Though the calculations represented in Figure 2 clearly indicate the stabilizing effect of nonlinearity they do not indicate the emergence of any local equilibrium state as the vortices develop downstream.

Further calculations were carried out for the same initial condition (3.2) but with different curvature distributions $\kappa(X)$. The three curvature distributions which we examined in detail and the values of a and G used in the calculations were :

$$\text{(a)} \quad \kappa(X) = \frac{1}{1 + (.02X - 2.4)}, \quad a = .16, \quad G = .1,$$

$$\text{(b)} \quad \kappa(X) = \frac{\sqrt{X}}{10}, \quad a = .2, \quad G = .23,$$

$$\text{and (c)} \quad \kappa(X) = \frac{\sqrt{X}}{10}\{1 + .2 \sin \frac{X}{40}\}, \quad a = .2, \quad G = .23.$$

The first curvature distribution was chosen because it corresponds to a flow over a hump such that the flow is only unstable over a finite interval. The second distribution was chosen since, as in the asymptotic theory of I, it gives a local Gortler number proportional to the fourth power of the local wavenumber. At relatively large values of X the local growth rate changes little with X and in the nonlinear regime we might expect to recover the results of III. The case (c) was chosen in order to obtain information about the possible influence of a small amplitude wall waviness on nonlinear Gortler vortices. The linear growth rate curves corresponding to (a), (b) and (c) and the initial conditions (3.1) are shown in Figure 4. It is interesting to see that the small amplitude waviness causes a significant difference between (b) and (c). We note that, whereas (a) is stable beyond $X \sim 140$, (b) and (c) remain unstable up to $X \sim 200$ beyond which the growth rates increase slowly.

In Figure 3a we have shown the energy functions E_0 and E_1 corresponding to $\Delta = .1, .2$ together with $a = .16$, $G = .0288$, and $\kappa(X) = \frac{X}{20}$. We see that the differences between the values of E_0, E_1 for $\Delta = .1$ and $\Delta = .2$ decreases with X. This is presumably because when X is large the effective wavenumber is also large and the analysis of III suggests that in this regime there exists a unique finite amplitude solution independent of its initial upstream form. However the calculation of III cannot be applied directly to the calculations reported here since they are restricted to an asymptotically small interval near to the neutral location. Nevertheless the short wavelength nonlinear theory of III does suggest that in this regime the origin of the disturbance is unimportant.

In Figures 3b,c we have shown the total downstream velocity component u_T at the spanwise locations $az = \pi/2, \pi, 2\pi$ together with the Blasius profile which exists in the absence of the vortices. The profiles shown correspond to $X = 300$ and we see that at this location there is very little difference between the profiles originating from $\Delta = .1$ and $\Delta = .2$. We further note that the values of u_T corresponding to $az = \pi/2$ are identical to those with $az = 3\pi/2$. Of particular interest is the fact that the $az = \pi$ profile has a strongly inflectional profile which is probably locally unstable to highly amplified Rayleigh instabilities. The location $az = \pi$ of course corresponds to the boundary between vortices where the motion of the fluid is away from the wall. We might therefore expect that such locations will be the most susceptible to the secondary instabilities which cause the onset of time dependence in the Gortler problem.

In Figures 3d,e,f,g we have shown the individual velocity components appropriate to the above situation with $\Delta = .2$. It can be seen that the disturbance is dominated by the fundamental and mean flow correction velocity components. We see that U_1 at $X = 300$ has a significantly different shape than the linear solution initially imposed on the flow at $X = 100$. We have no physical explanation of the nonlinear mechanism which produces this distortion.

In Figure 5 we have shown the energy functions appropriate to the curvature distribution (a). The linear eigenfunction was obtained by inserting (3.2) at $X = 55.$ and integrating until $X = 85.$ where the nonlinear terms were turned on.

The initial disturbance amplitudes were taken to be = .1 and = .15. We see that the energy of the disturbance is again almost completely confined to the fundamental and mean flow correction. The maximum value of the disturbance energies E_1, E_2, E_3 occur close to the position where the linear growth rate (a) of Figure is zero. In contrast the maximum of E_0 occurs at a higher value of X. This suggests that the results of Figure 5 are dominated by the interaction between the basic Blasius boundary layer and the fundamental component of the disturbance and never reach any 'local' nonlinear equilibrium state.

In Figure 6 the results corresponding to the case (b) are shown. The nonlinear terms were again turned on at $X = 85.$ after integrating (3.2) from $X = 55.$ and four calculations corresponding to $\Delta = .05, .1, .15, .20$ were carried out. Figures 6a,b,c show the evolution in X of the energy functions E_0, E_1 and E_2 for this situation. The functions E_0 and E_1 appear to approach limiting values essentially independent of Δ whilst E_2 initially increases before decaying at sufficiently large values of X. This suggests that as the vortices develop into a region where the effective Gortler number G_x and the effective wavenumber a_x satisfy $G_x \sim a_x^4$, $a_x >> 1$ the asymptotic structure found in III is qualitatively recovered. In the latter calculation it was found that small wavelength Gortler vortices develop through a 'mean-field' interaction between the fundamental and mean flow correction. A quantitative comparison between our results and III is not possible since the asymptotics of III was restricted to a $O(a^{-1})$ neighbourhood of the neutral value of X.

The downstream development of the individual velocity components in the above calculation is shown in Figure 7. It can be seen that the characteristic nonlinear shape of U_1 shown in Figure 3d for the $\kappa = \frac{X}{20}$ calculation is reproduced at sufficiently large values of X. The value of X required to produce this characteristic shape decreases with the size of the initial amplitude. Similarly the mean flow corrections calculated have a similar shape to that shown in Figure 3d and that produced by the asymptotic theory of III. Indeed the mean flow corrections calculated for the cases (a), (b), and (c) together with the case $\kappa = \frac{X}{20}$ all had the same characteristic shape. Similarly the downstream velocity component was always found to increase away from the wall, reach a maximum and then decay to zero. Since this velocity component and the mean flow correction are always much larger than the other X velocity components it follows that the spanwise distribution of u_T the total downstream velocity component will always be similar to those shown in Figure 3b. In Figure 8 we have shown how these profiles develop in X for the case $\Delta = .05$ together with the corresponding undisturbed profile. Again the $az = \pi$ profiles become highly inflectional and are presumably highly unstable to Rayleighs instabilities of the type discussed by, for example, Cowley and Tufty (1986). We believe that the development of these highly inflectional profiles at the spanwise locations where upwelling occurs is the most likely source of the time-dependent secondary instabilities which steady Gortler vortices are known to suffer, see, for example, Aihara (1965).

Finally in Figure 9 we have shown the energy distributions for the case (c). The calculations were again performed by integrating (3.2) from $X = 55.$ to $X = 85.$ where the nonlinear terms were turned on. A comparison between Figures 9a,b,c and Figures 6a,b,c shows that the wall waviness does not have a significant effect on the energy distributions for $\Delta = .05$. However the solutions for the larger amplitude $\Delta = .15$ suggest that the waviness increases the energy of the disturbance up to $X \tilde{} 200$. The computational expense of these calculations prevented us from determining whether a small amplitude waviness always leads to a destabilization of the boundary layer.

REFERENCES

1. Bennett, J. and P. Hall, "On the secondary instability of Taylor-Gortler vortices in fully developed flows," submitted to J. Fluid Mech., 1986.

2. Floryan, J. and W. S. Saric, "Stability of Gortler vortices in boundary layers," AIAA paper No. 79-1497.

3. Hall, P., "Taylor-Gortler instabilities in fully developed or boundary layer flows: Linear theory," J. Fluid Mech., Vol. 124, 1982a, p. 475.

4. Hall, P., "On the nonlinear evolution of Gortler vortices in growing boundary layers," J. Inst. Math. Applics., Vol. 29, 1982b, p. 173.

5. Hall, P., "The linear development of Gortler vortices in growing boundary layers," J. Fluid Mech., Vol. 130, 1983, p. 41.

6. Hammerlin, G., "Zur theorie der dreidimensionalen instabilitat laminar Grenzschichten," Z. Angew. Mach. Phys., 1956, Vol. 1, p. 156.

7. Herbert, T., "On the stability of a boundary layer on a curved wall," Arch. Mech., Vol. 28, 1976, p. 1039.

8. Tutty, O. R. and S. J. Cowley, "On the stability and numerical solution of the unsteady boundary layer equations," J. Fluid Mech., Vol. 168, p. 431.

LEGENDS

Figure 1 The growth rate σ_1 for the wall $\kappa = \frac{X}{20}$, for Δ = .05, .1, .15, .2

Figure 2 The growth rate σ_2 for the wall $\kappa = \frac{X}{20}$, for Δ = .05, .1, .15, .2

Figure 3a The energy distributions E_0, and E_1 for $\kappa = \frac{X}{20}$, and Δ = .1, .2 .

Figure 3b The total X velocity component at different spanwise locations for X = 300., $\kappa = \frac{X}{20}$, Δ = .1 .

Figure 3c The total X velocity component at different spanwise locations for X = 300., $\kappa = \frac{X}{20}$, Δ = .2 .

Figure 3d The X velocity components at X = 300. for $\kappa = \frac{X}{20}$, Δ = .2 .

Figure 3e The Y velocity components at X = 300. for $\kappa = \frac{X}{20}$, Δ = .2 .

Figure 3f The Z velocity components at X = 300. for $\kappa = \frac{X}{20}$, Δ = .2 .

Figure 3g The mean flow correction at X = 300. for $\kappa = \frac{X}{20}$, Δ = .2 .

Figure 4 The growth rates for the cases (a), (b), and (c) respectively in the linear regime.

Figure 5a The energy function E_0 for (a) with Δ = .1, .15 .

Figure 5b The energy function E_1 for (a) with = .1, .15 .

Figure 5c The energy function E_2 for ((a) with = .1, .15 .

Figure 5d The energy function E_3 for (a) with $\Delta = .1, .15$.

Figure 6a The energy function E_0 for (b) with $\Delta = .05, .1, .15, .2$.

Figure 6b The energy function E_1 for (b) with $\Delta = .05, .1, .15, .2$.

Figure 6c The energy function E_2 for (b) with $\Delta = .05, .1, .15, .2$.

Figure 7a The X velocity component U_1 for (b) with $\Delta = .05$.

Figure 7b The X velocity component U_1 for (b) with $\Delta = .1$.

Figure 7c The X velocity component U_1 for (b) with $\Delta = .15$.

Figure 7d The X velocity component U_1 for (b) with $\Delta = .20$.

Figure 7e The X velocity component U_0 for (b) with $\Delta = .05$.

Figure 7f The X velocity component U_0 for (b) with $\Delta = .1$.

Figure 7g The X velocity component U_0 for (b) with $\Delta = .15$.

Figure 7h The X velocity component U_0 for (b) with $\Delta = .2$.

Figure 8a The total X velocity component for (b) with X = 125, 165, 205, 245, and $\Delta = 0$.

Figure 8b The total X velocity component for (b) with X = 125, 165, 205, 245, and $\Delta = .05$, $az = \pi/2$.

Figure 8c The total X velocity component for (b) with X = 125, 165, 205, 245, and $\Delta = .05$, $az = \pi$.

Figure 8d The total X velocity component for (b) with X = 124, 165, 205, 245, and $\Delta = .05$, $az = 2\pi$.

Figure 9a The energy function E_0 for (c) with $\Delta = .05, .15$.

Figure 9b The energy function E_1 for (c) with $\Delta = .05, .15$.

Figure 9c The energy function E_2 for (c) with $\Delta = .05, .15$.

Figure 1

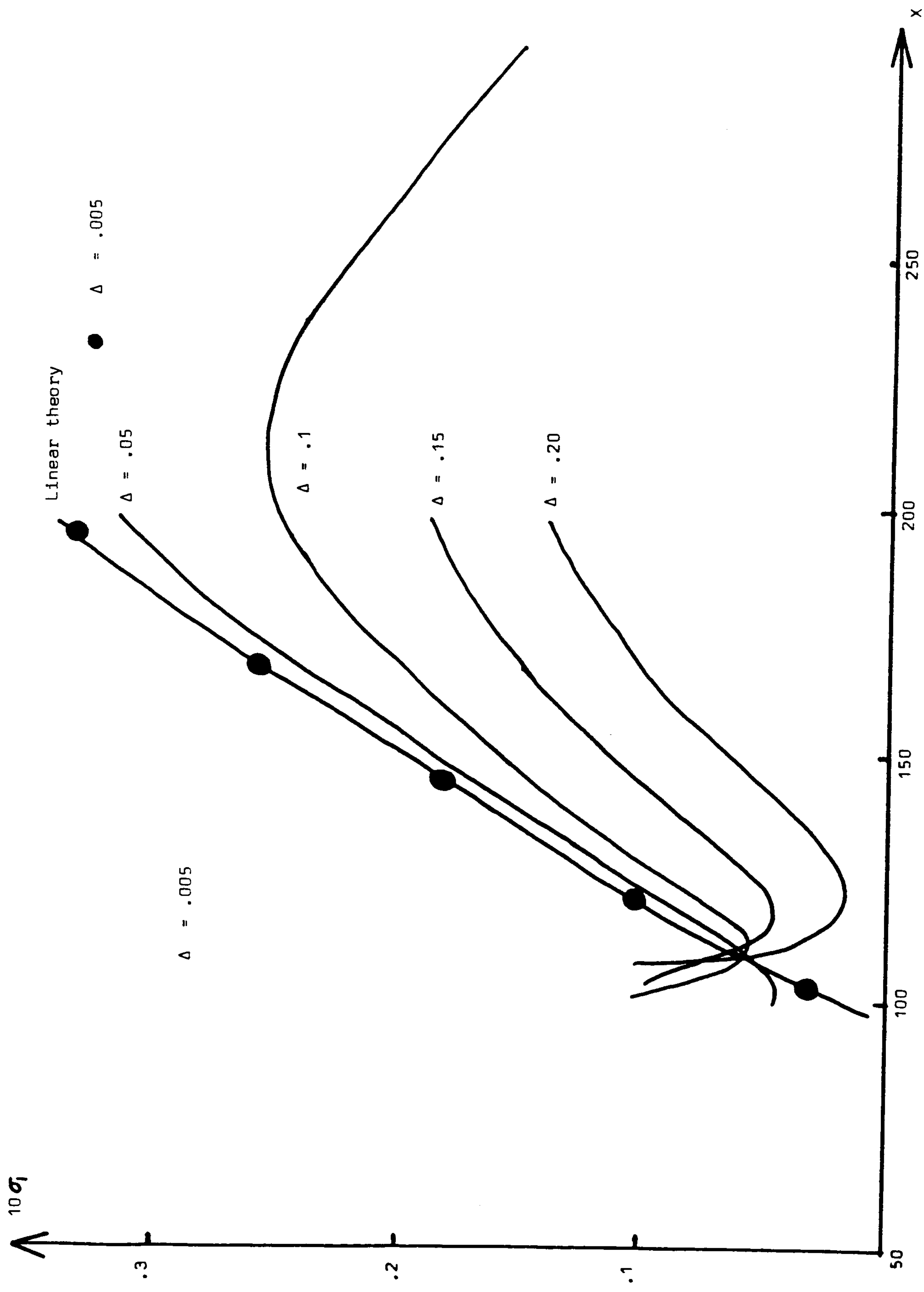

$10\sigma_1$
.3
.2
.1
50
100
150
200
250
x
Linear theory
● Δ = .005
Δ = .05
Δ = .1
Δ = .15
Δ = .20
Δ = .005

Figure 2

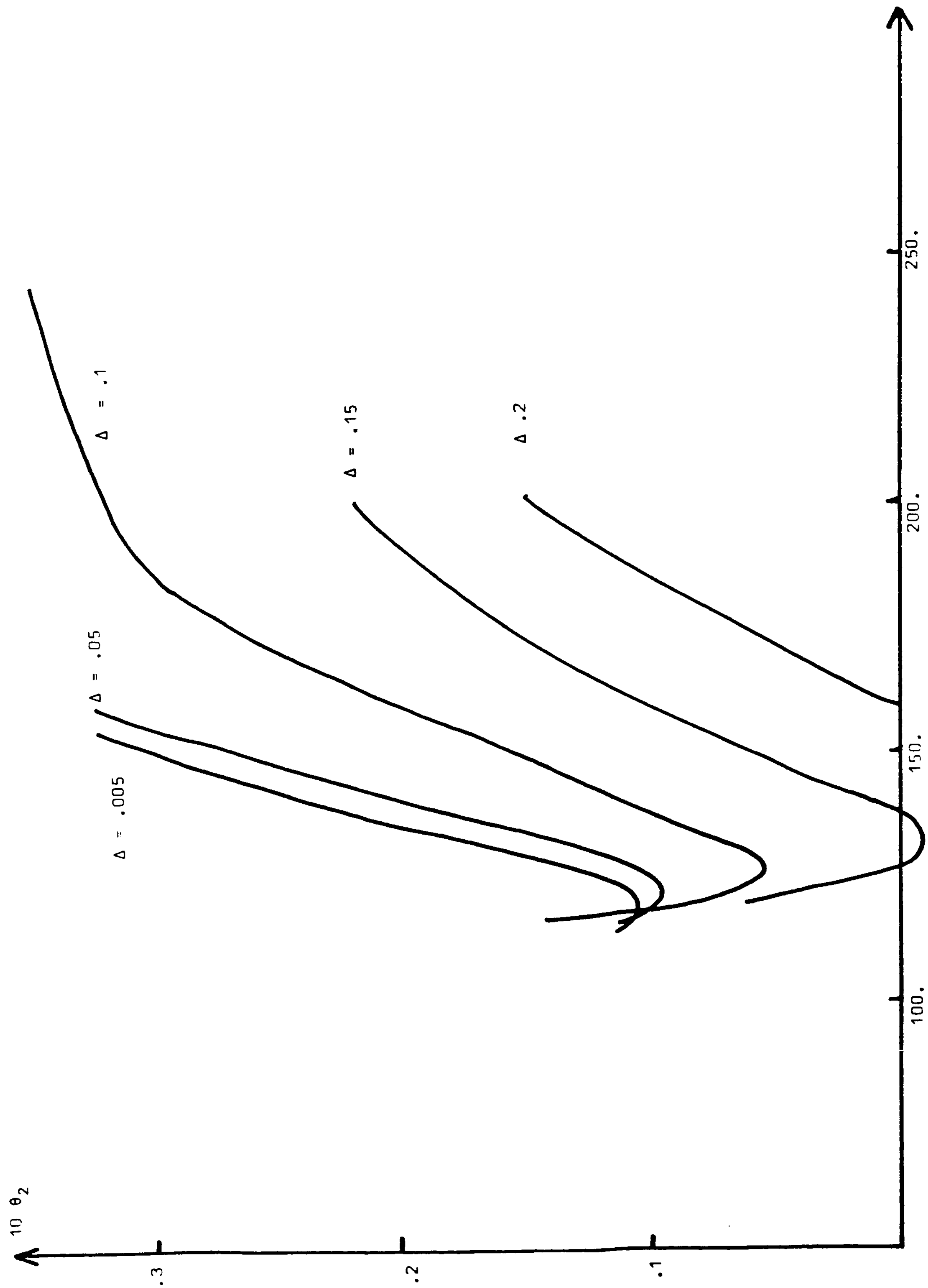

Figure 3a

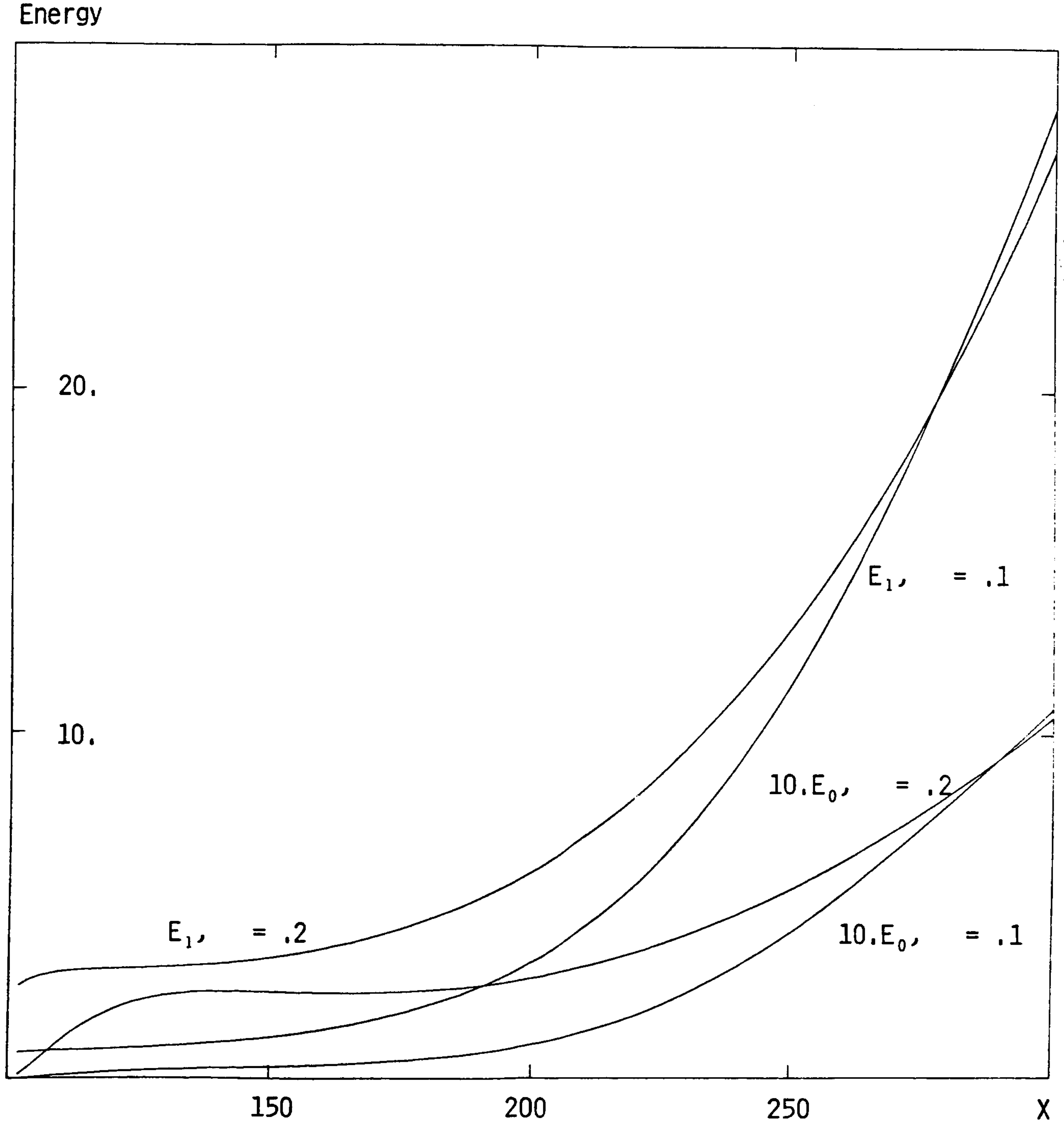

Figure 3b

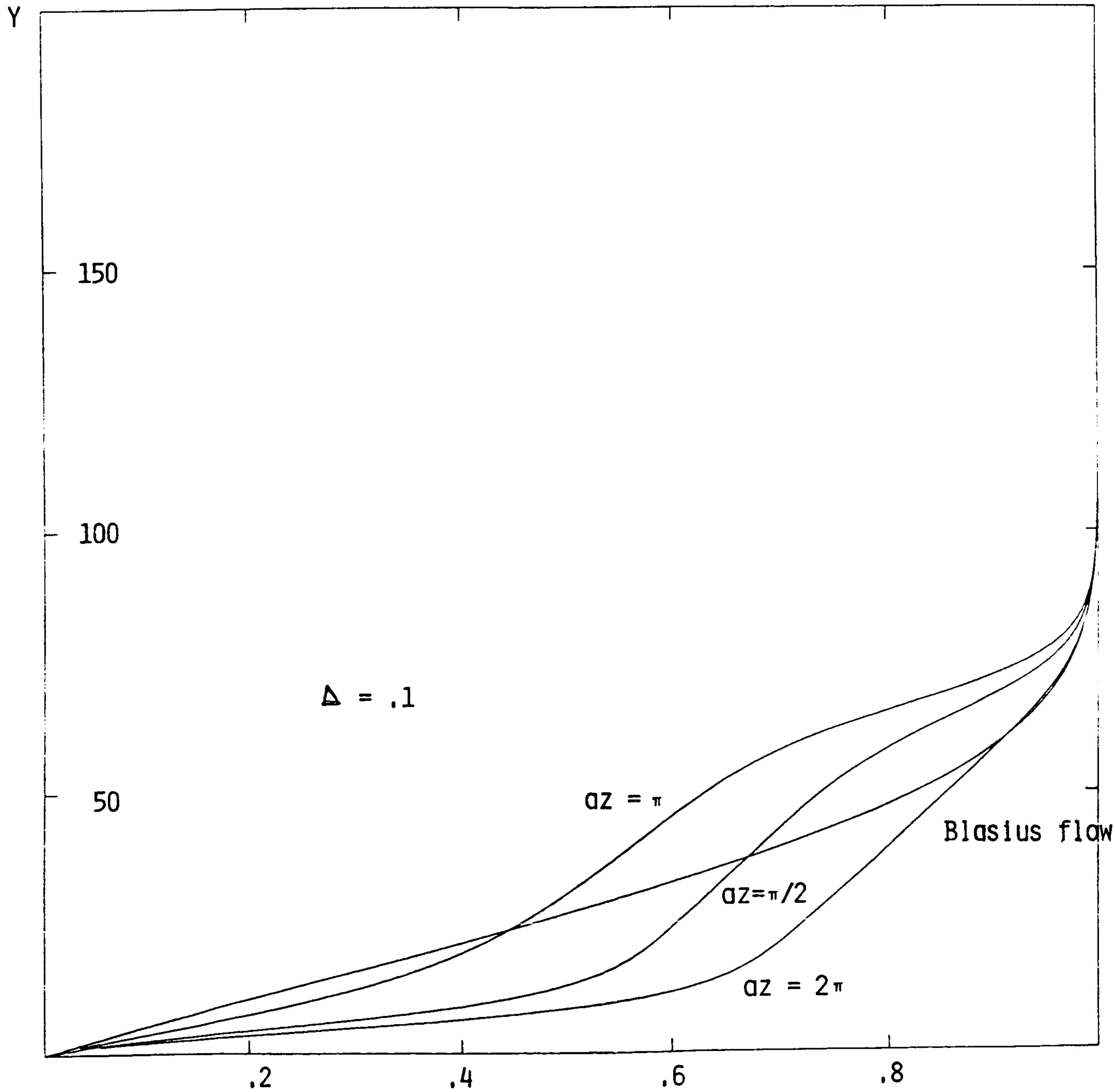

Figure 3c

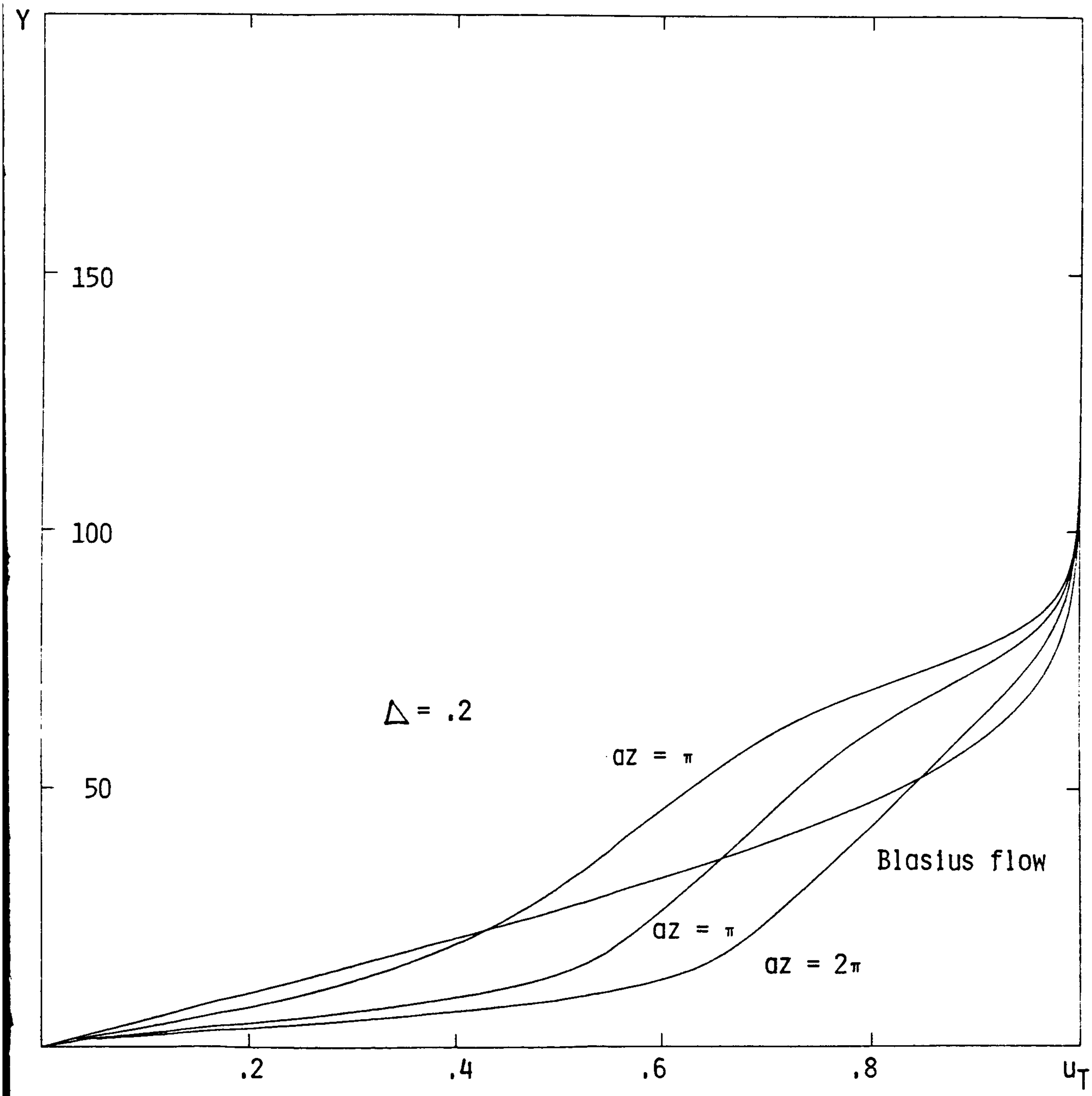
Y
150
100
50
$\Delta = .2$
$\alpha z = \pi$
Blasius flow
$\alpha z = \pi$
$\alpha z = 2\pi$
.2
.4
.6
.8
u_T

Figure 3d

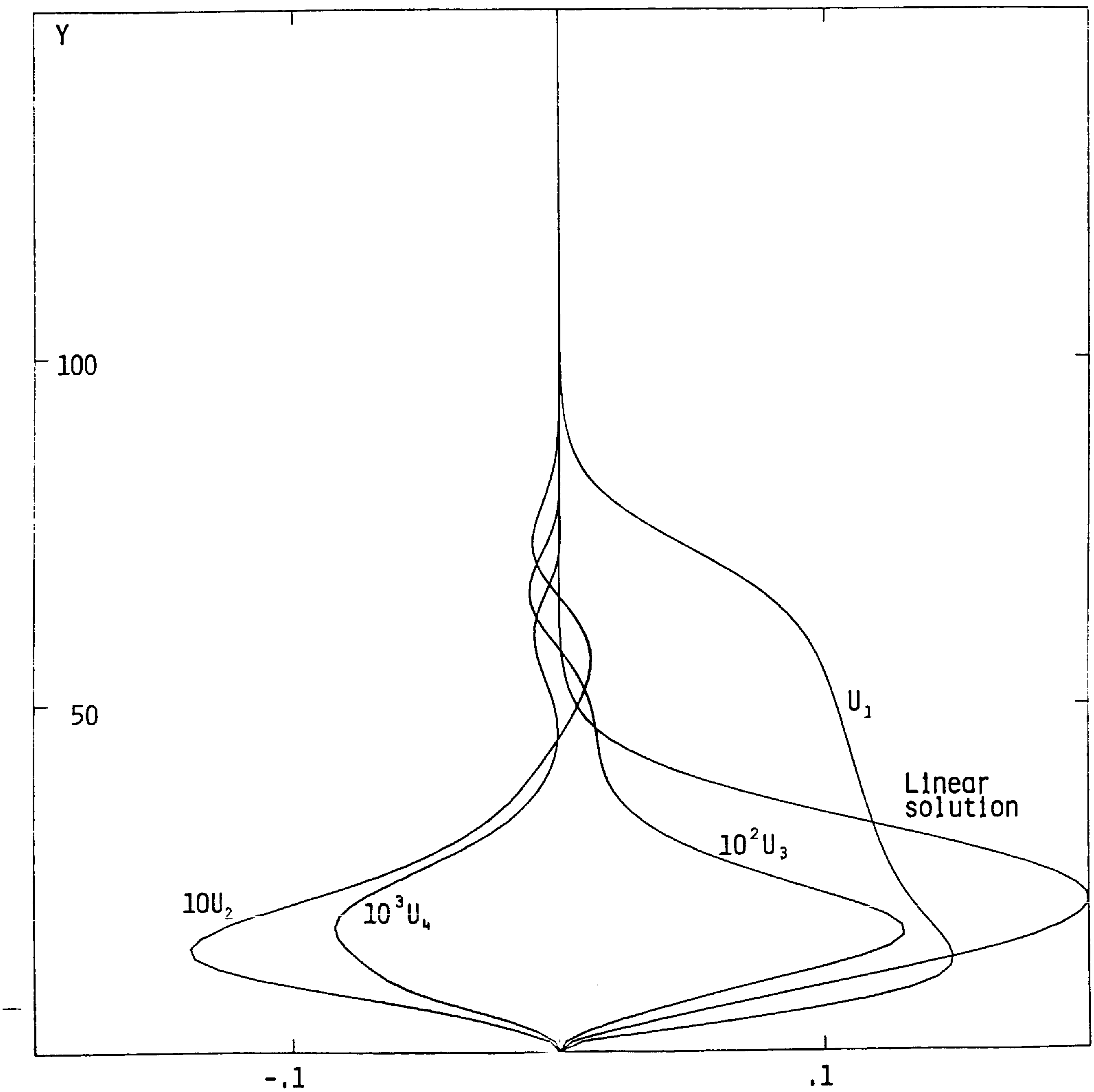

Figure 3e

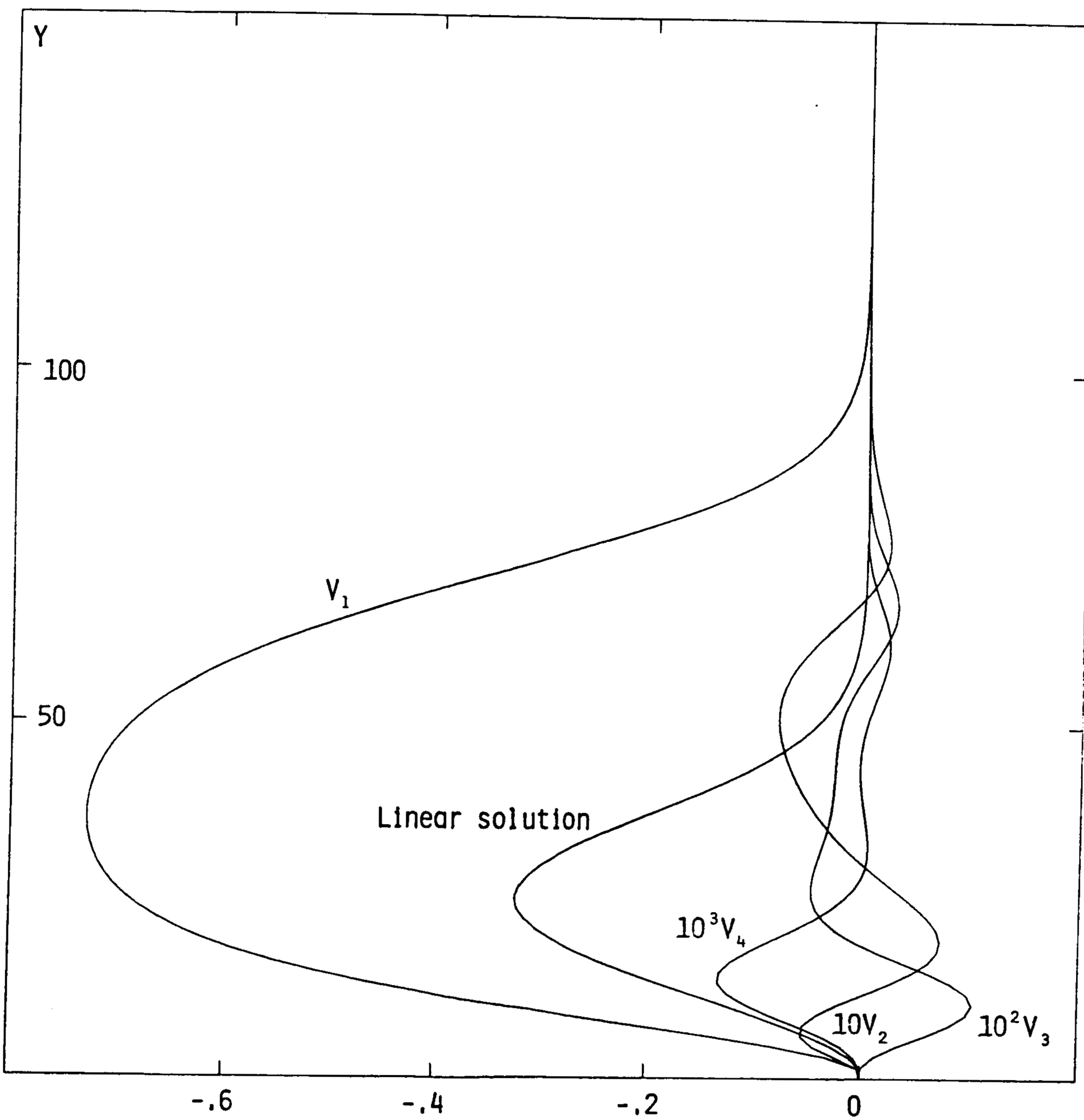

Figure 3f

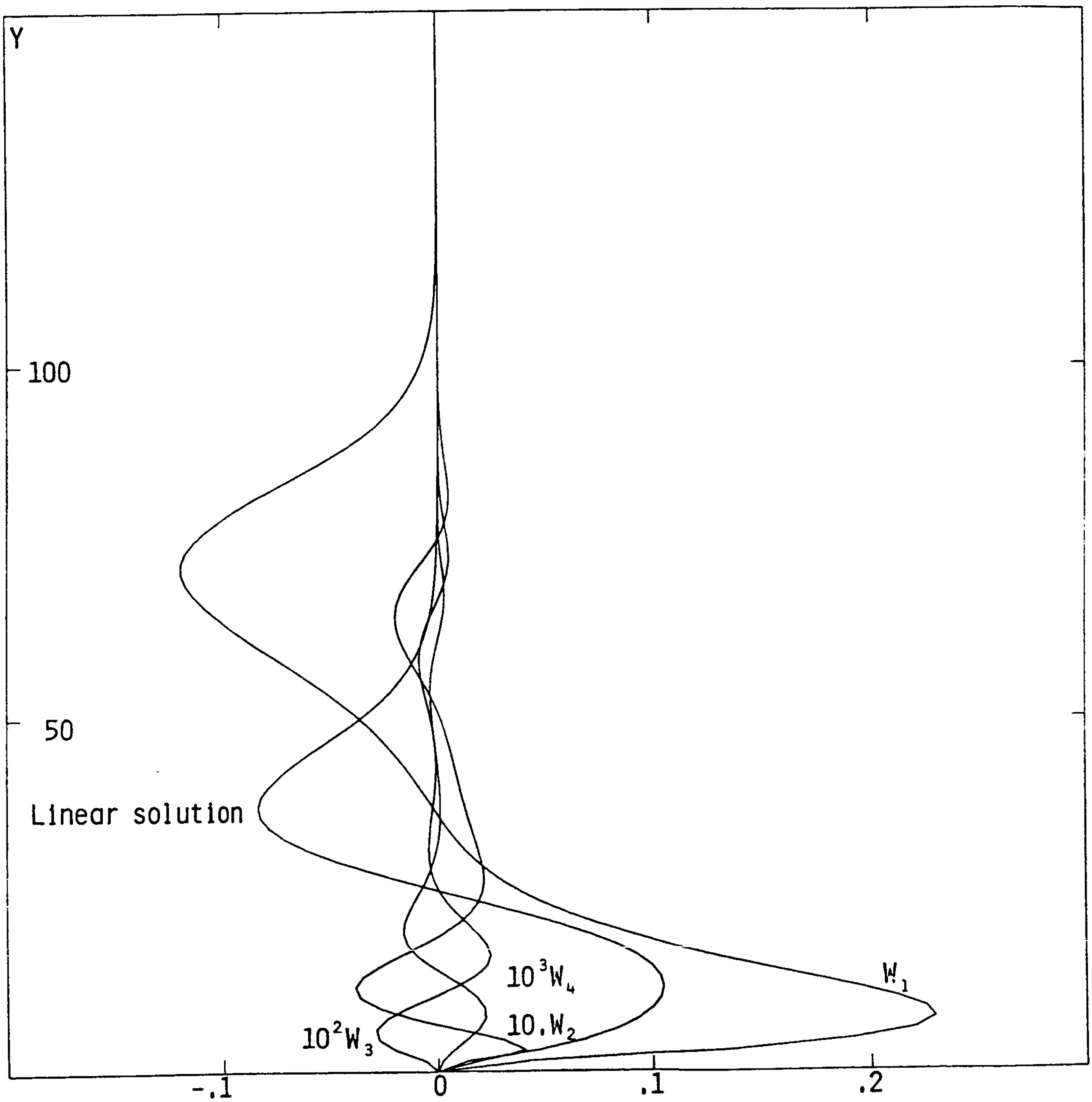

Figure 3g

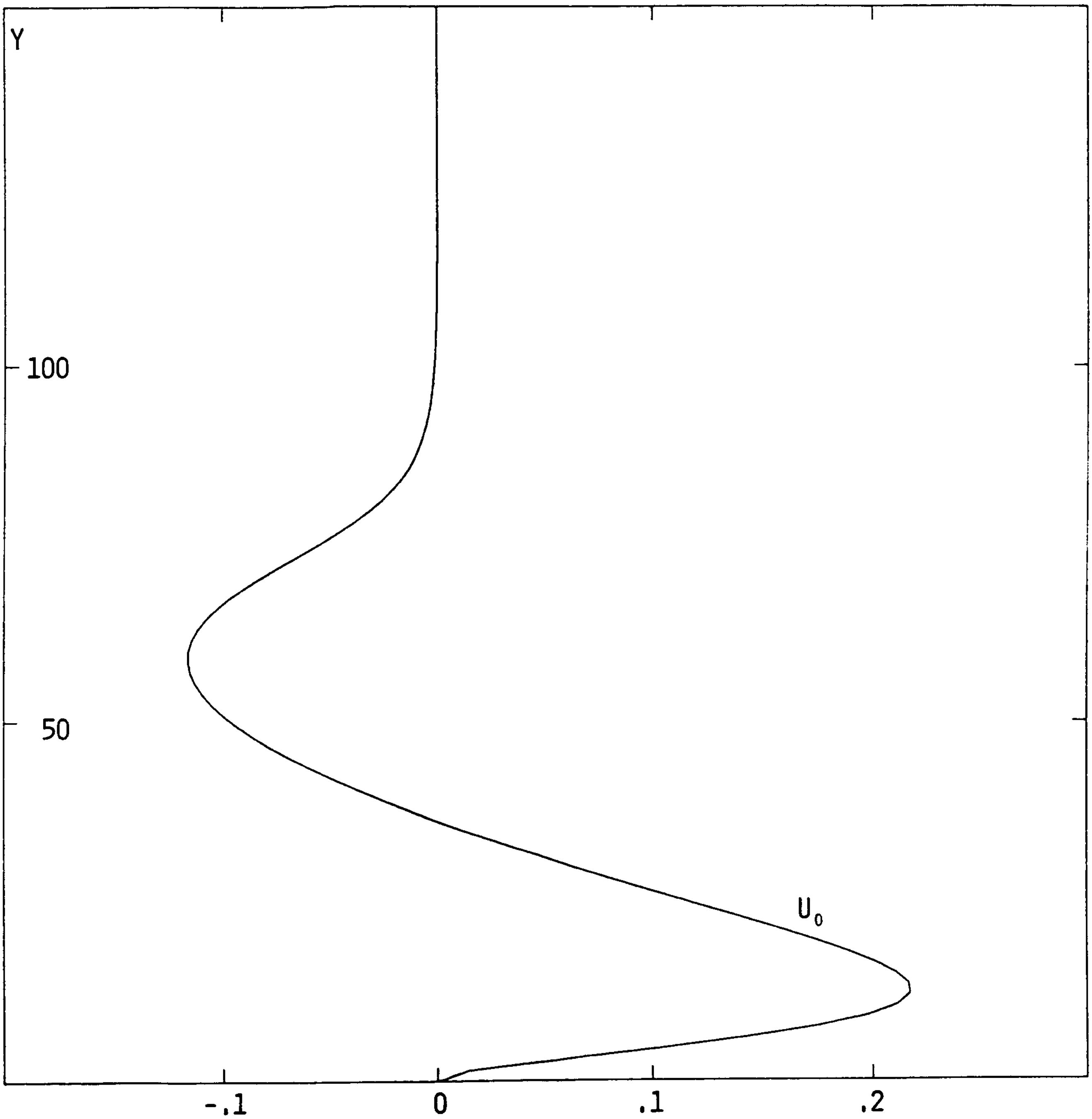

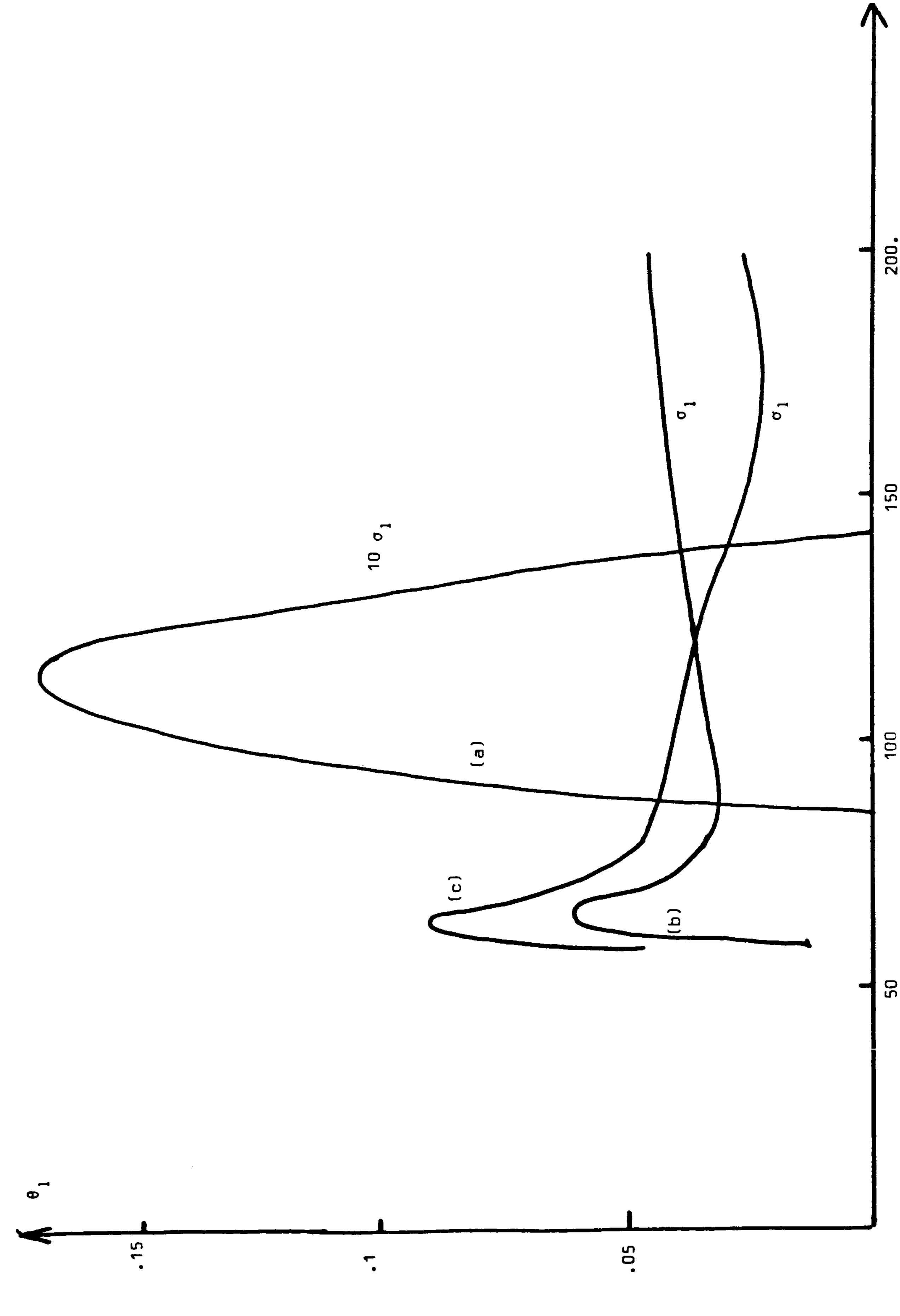

Figure 4

Figure 5a

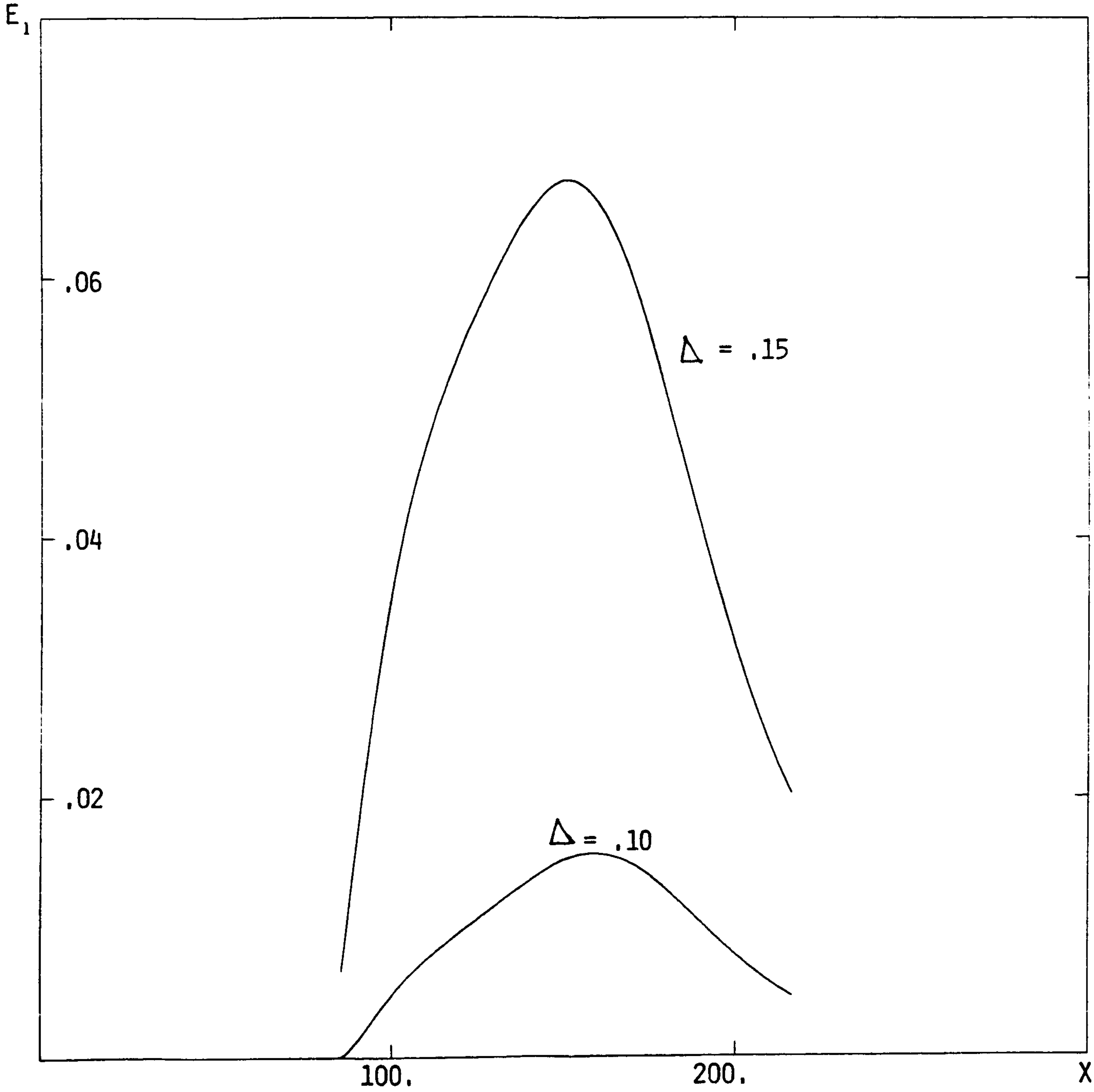

Figure 5b

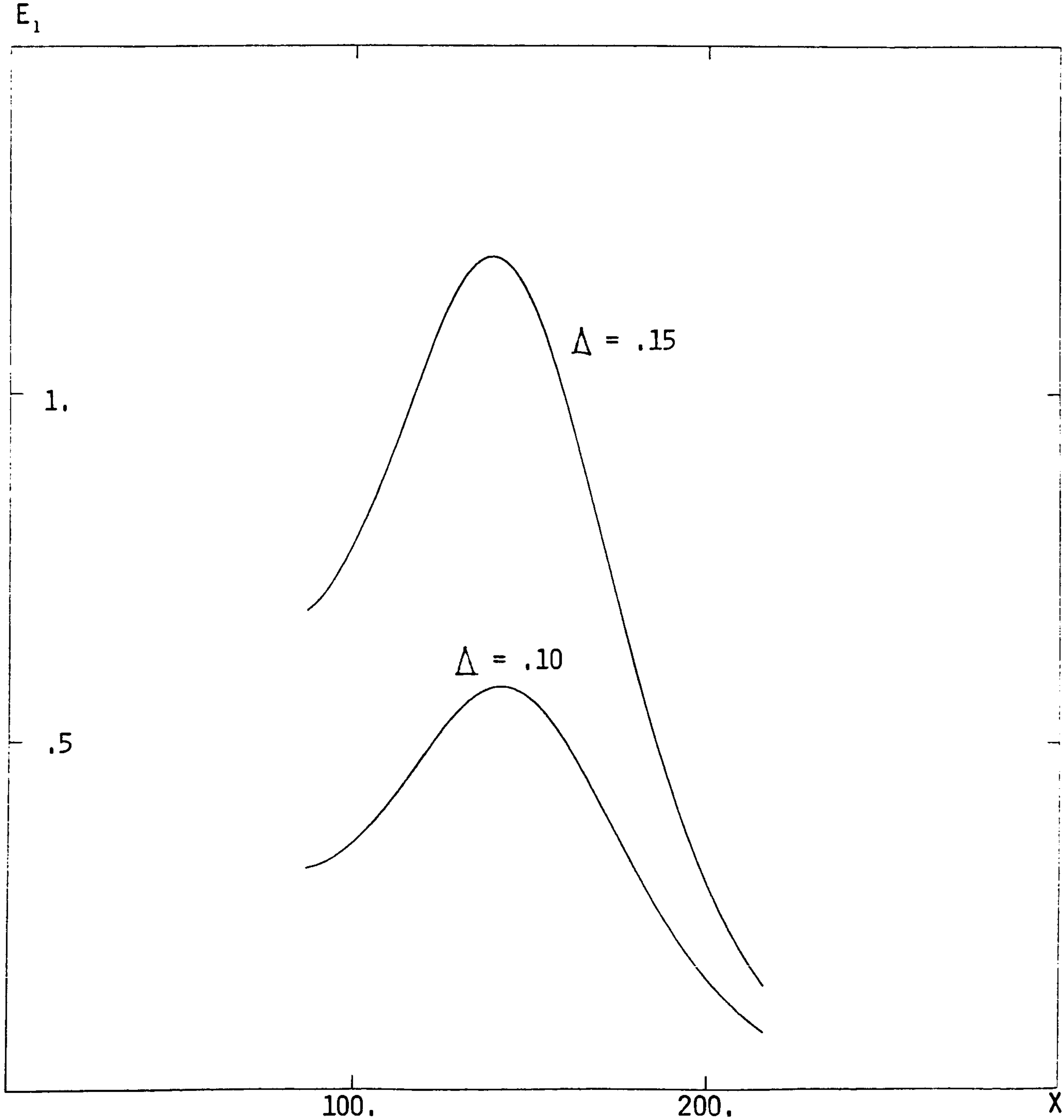

Figure 5c

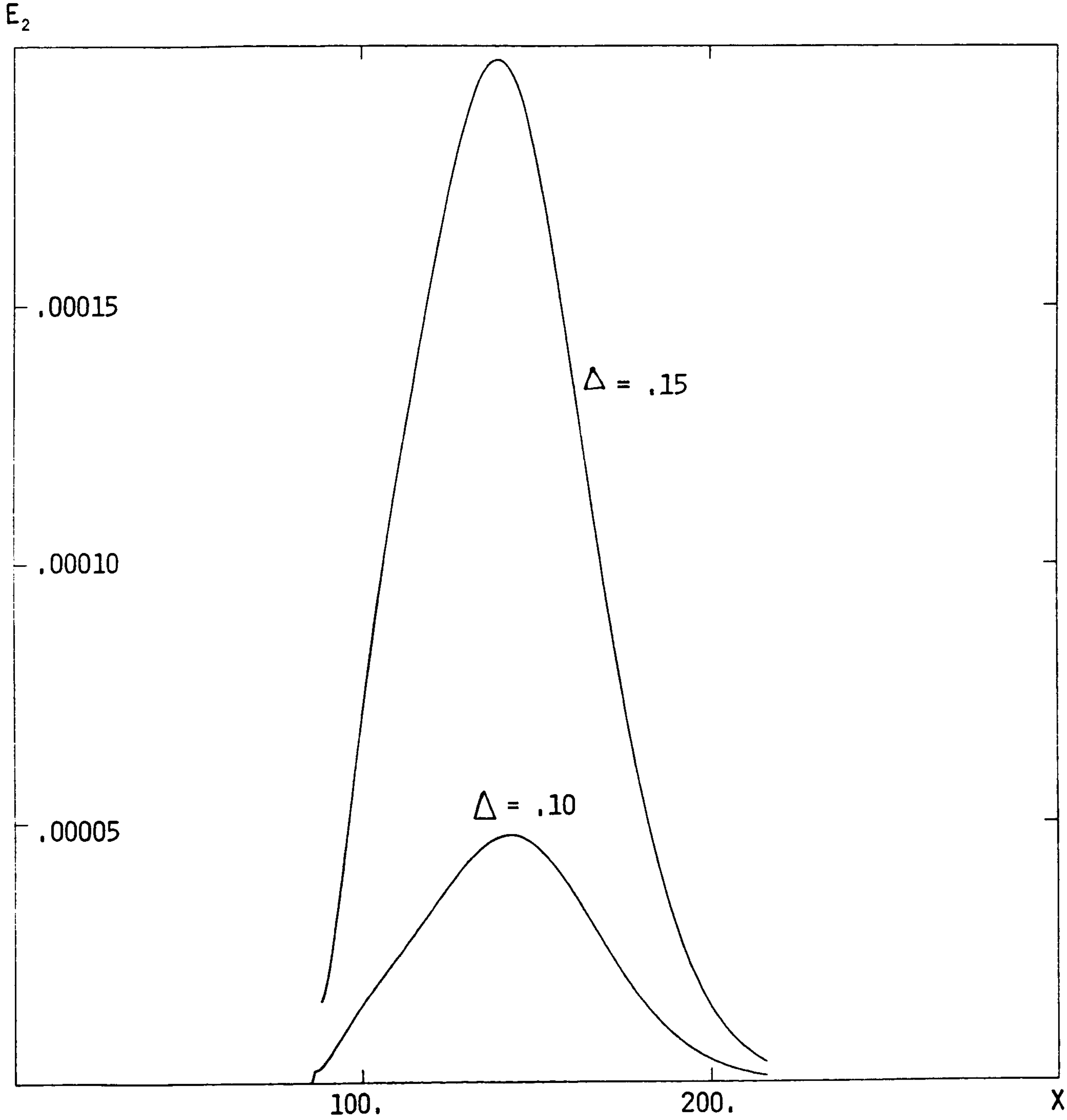

Figure 5d

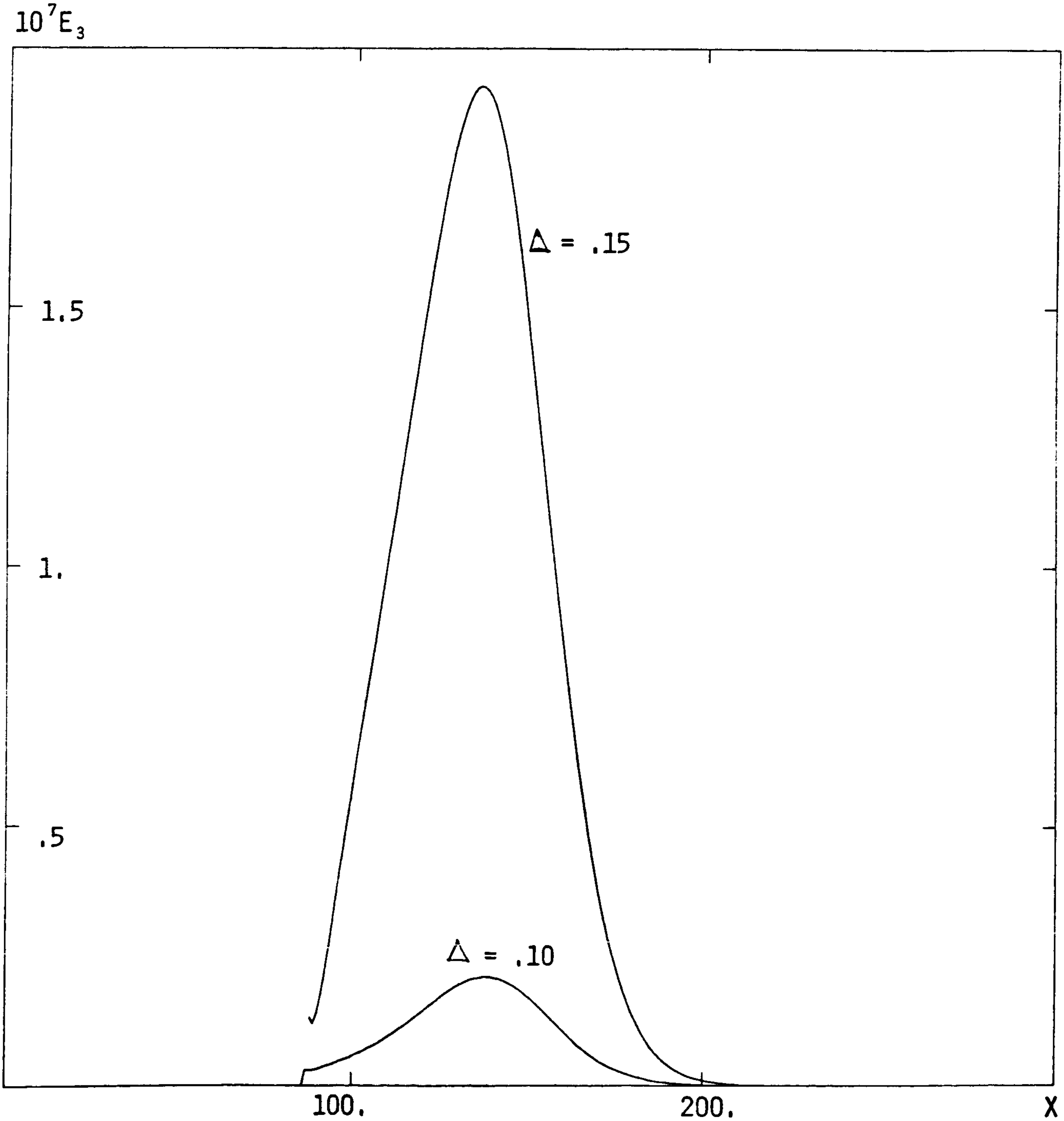

Figure 6a

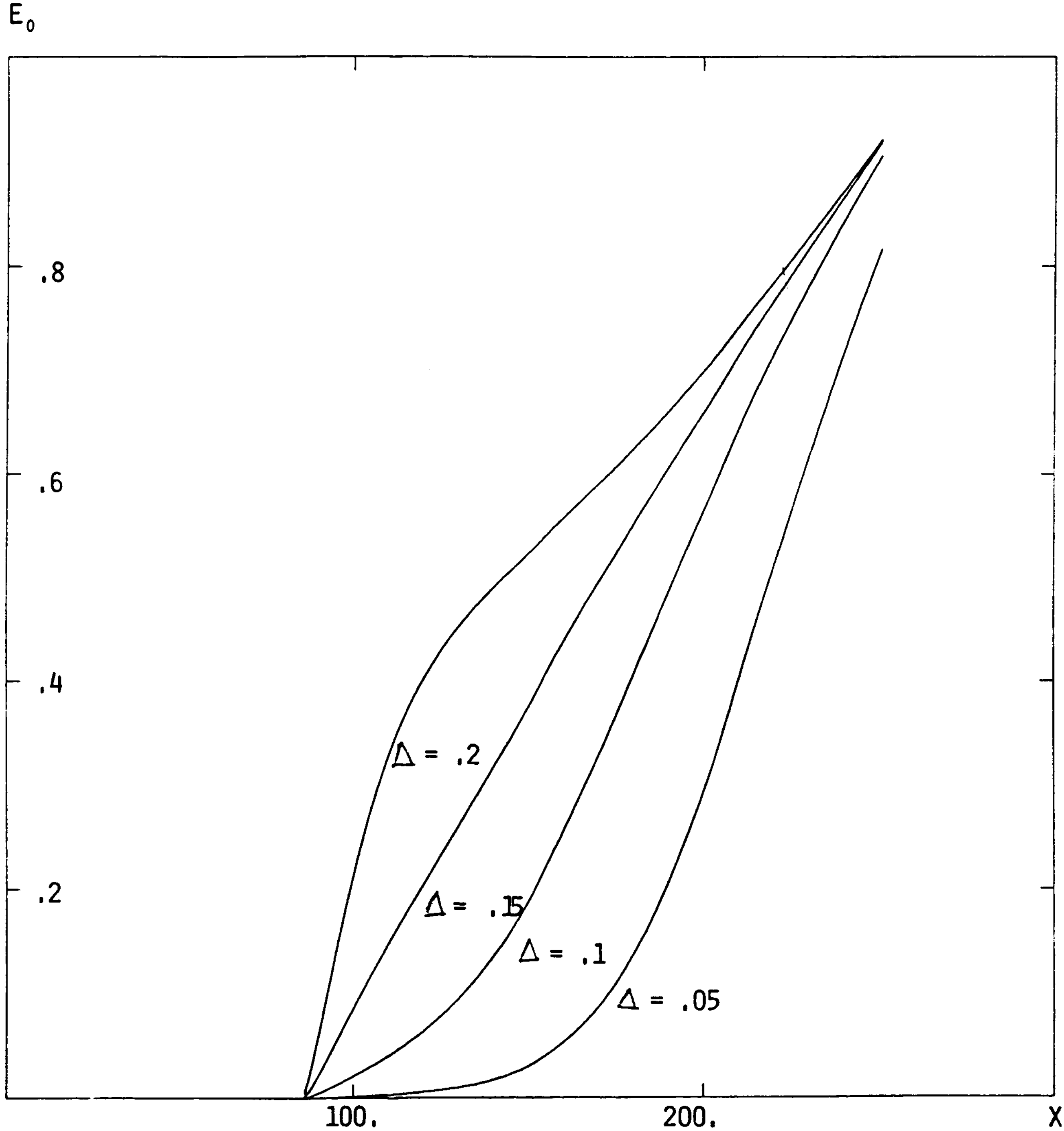

Figure 6b

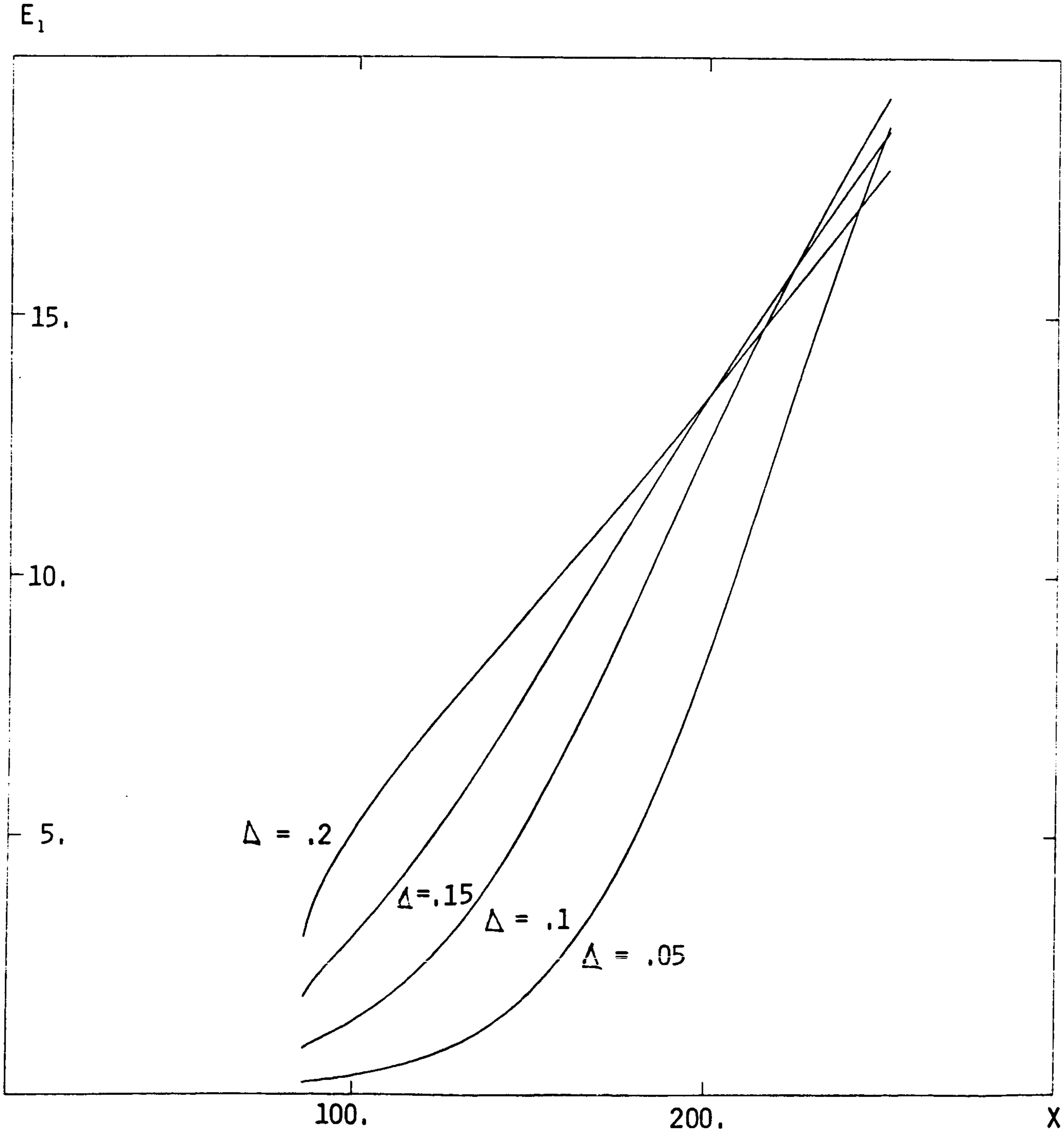

Figure 6c

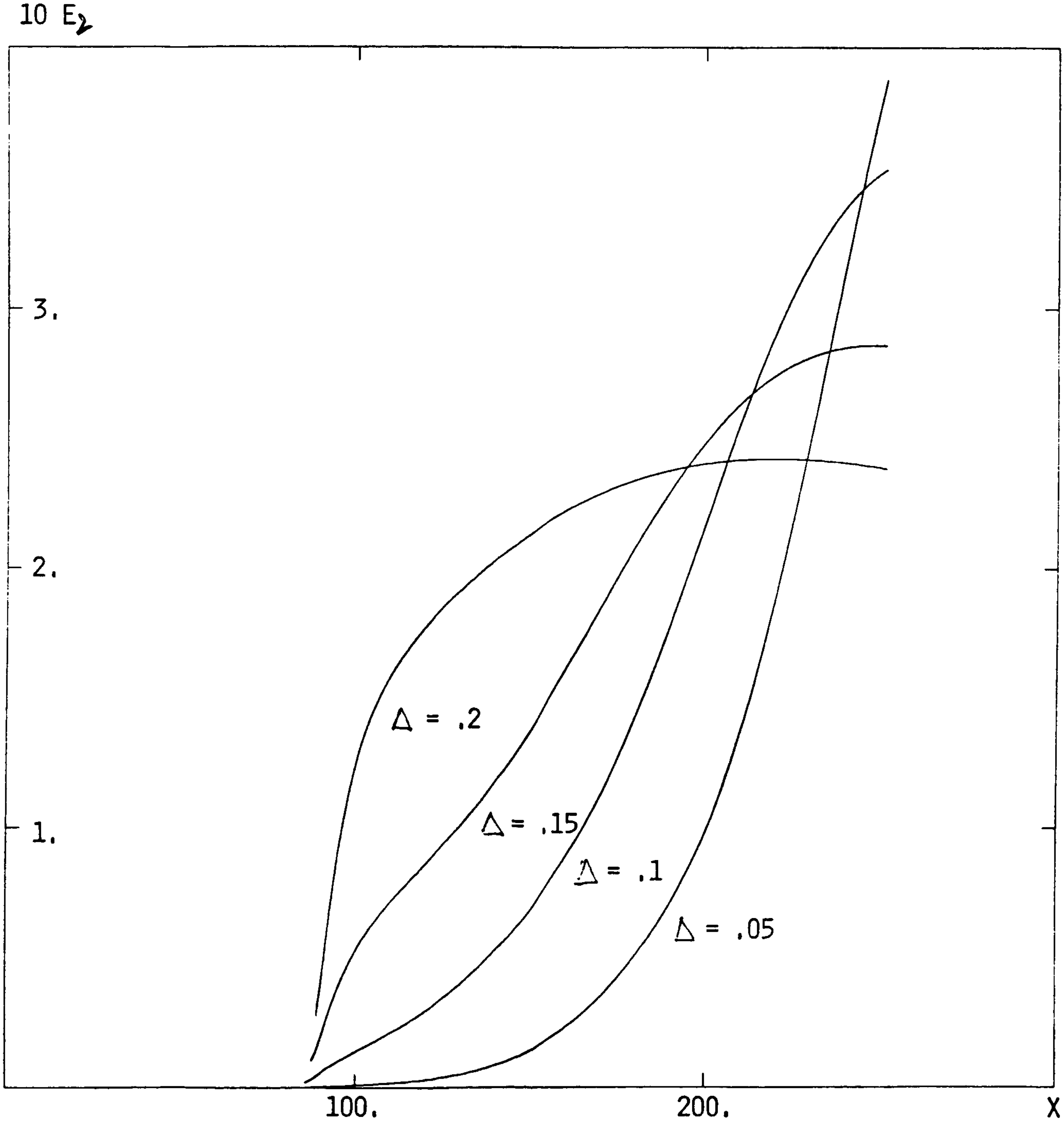

Figure 7a

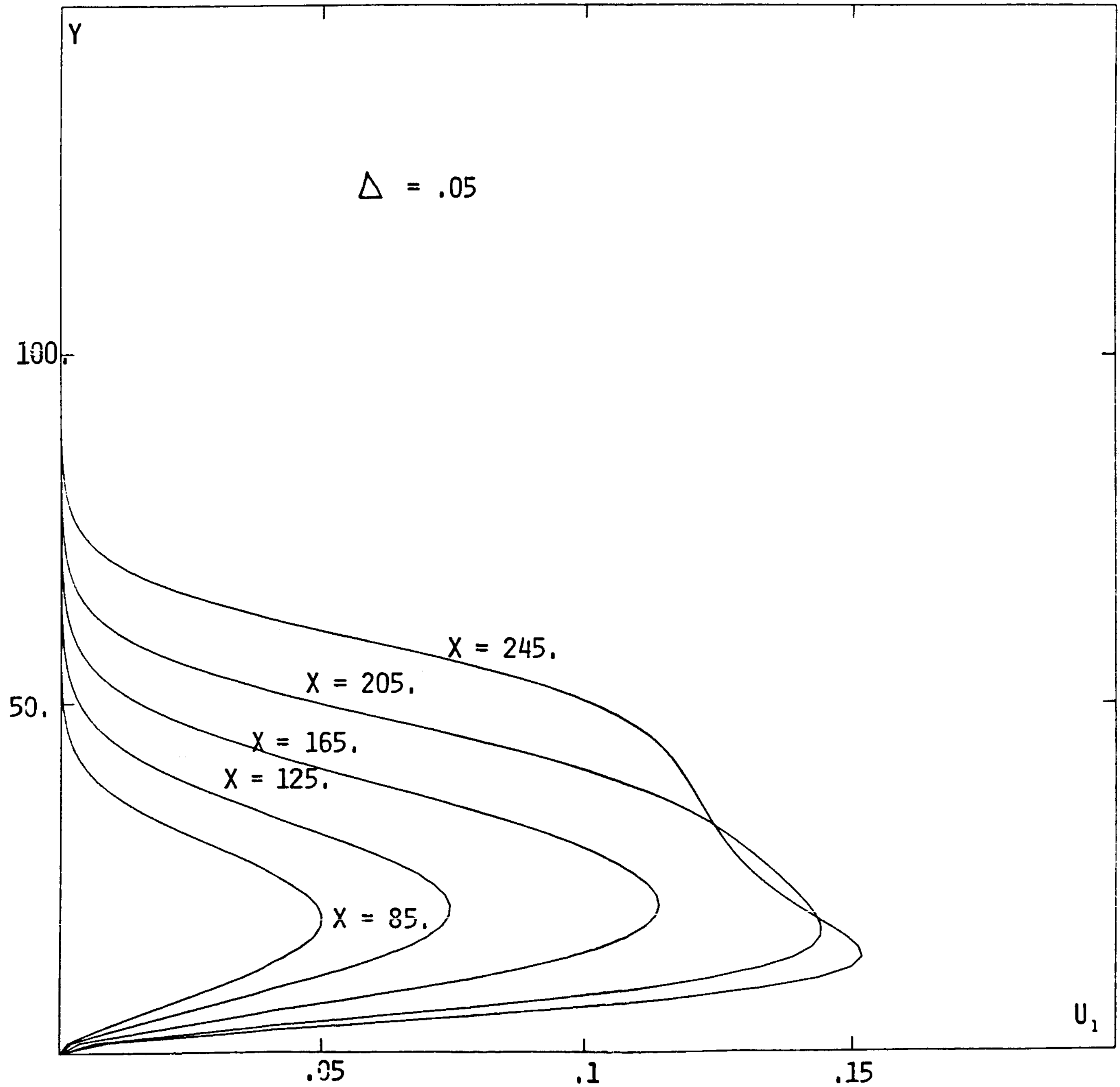

Figure 7b

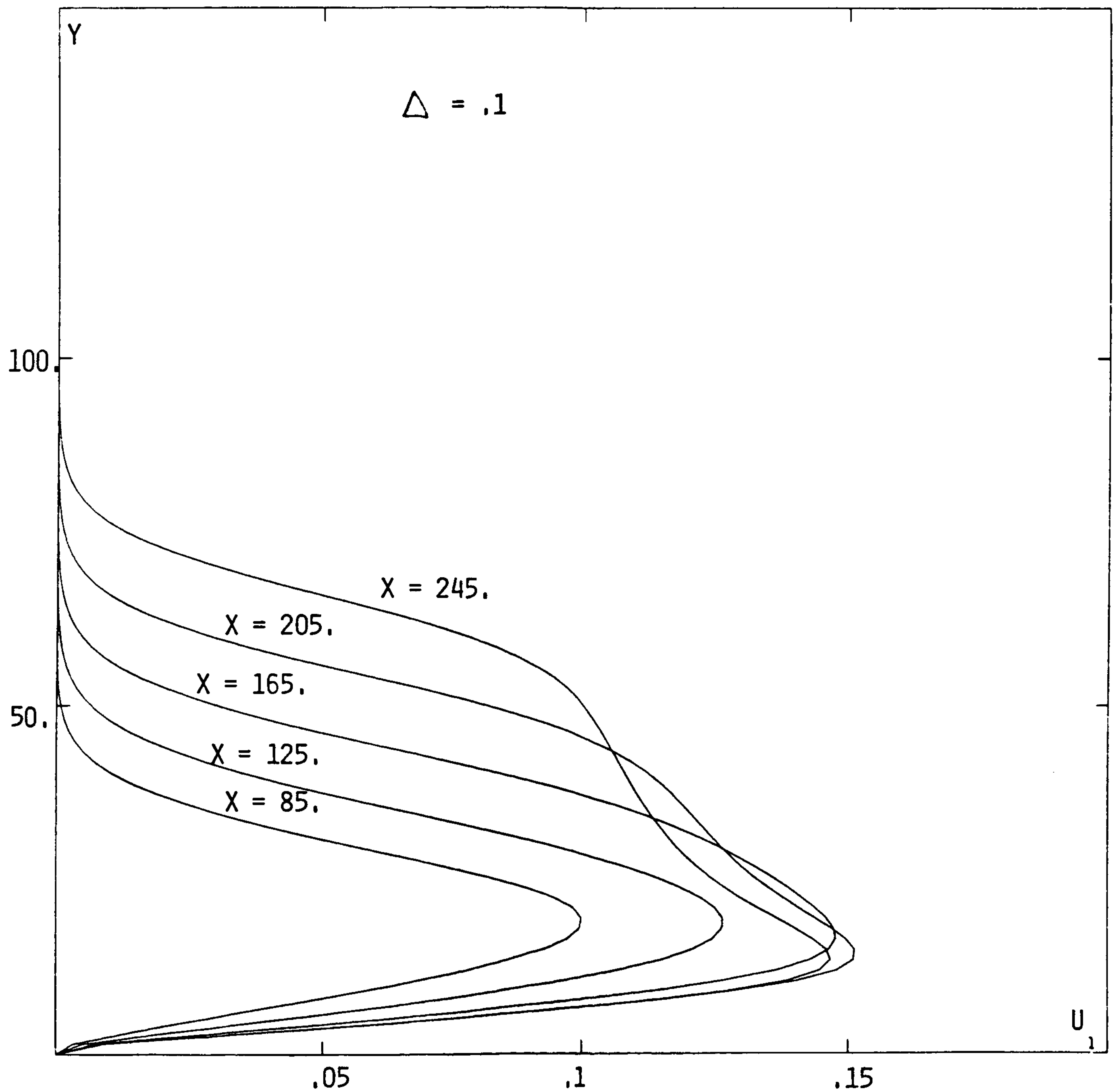

Figure 7c

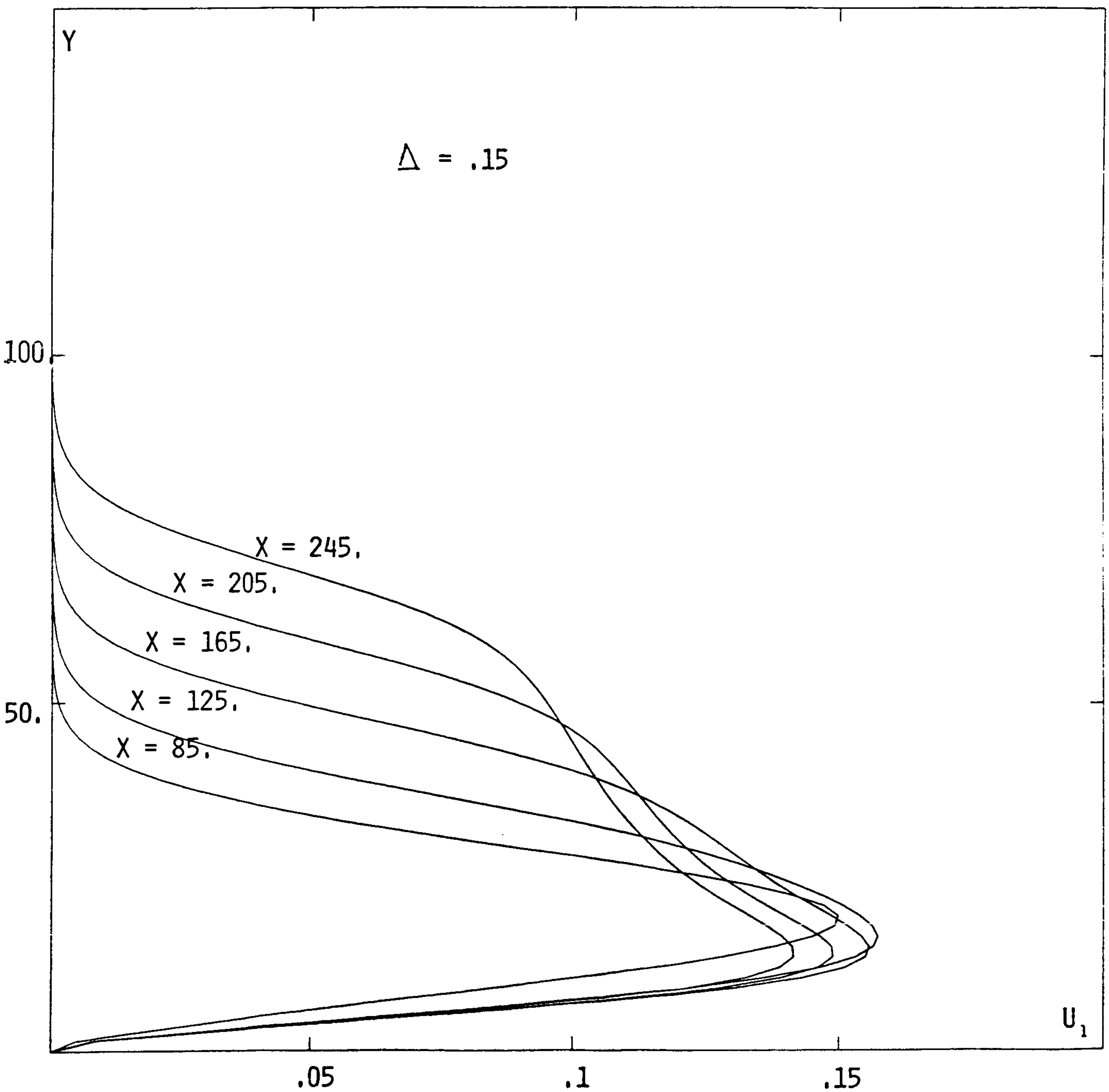

Figure 7d

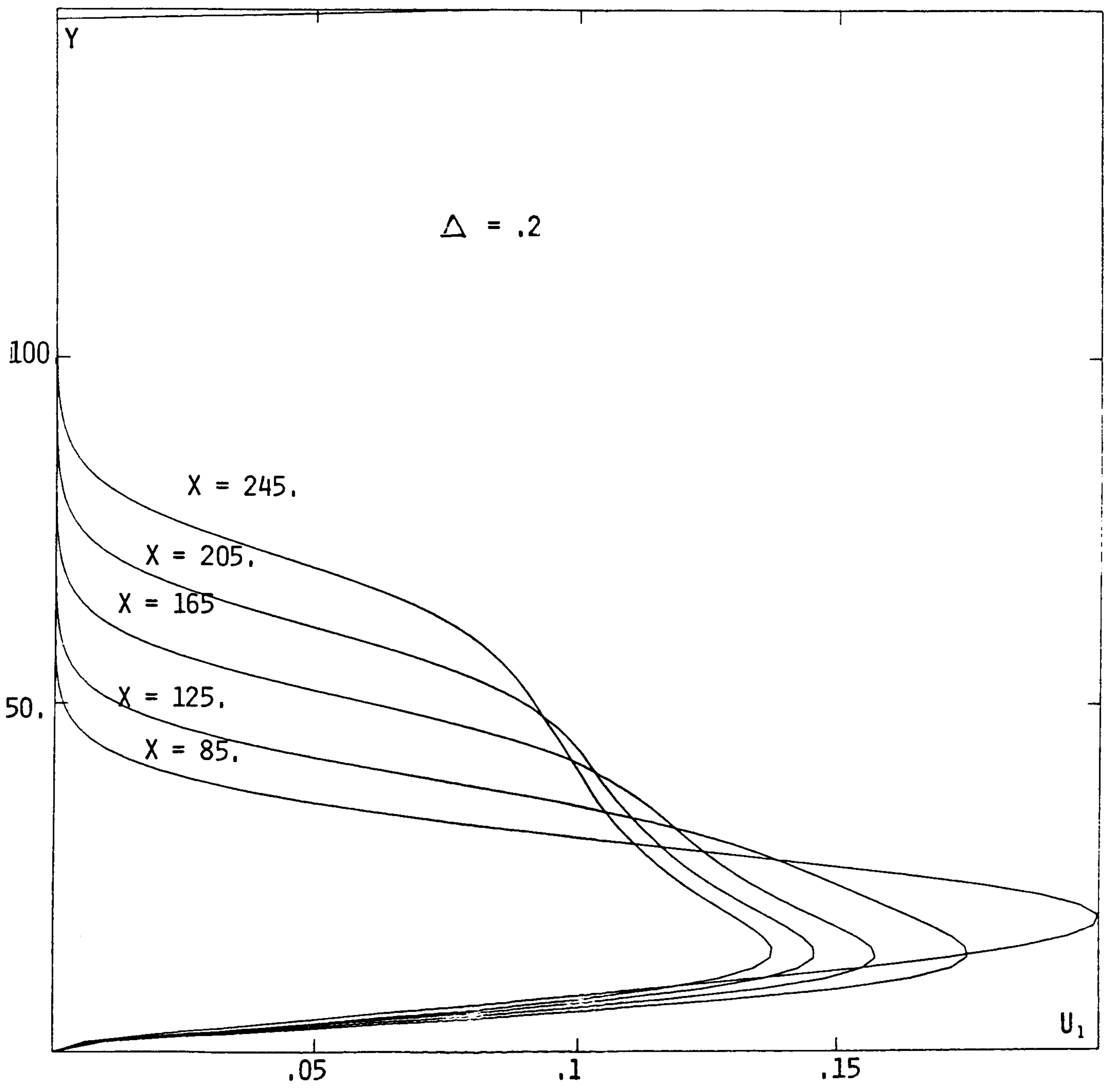

Figure 7e

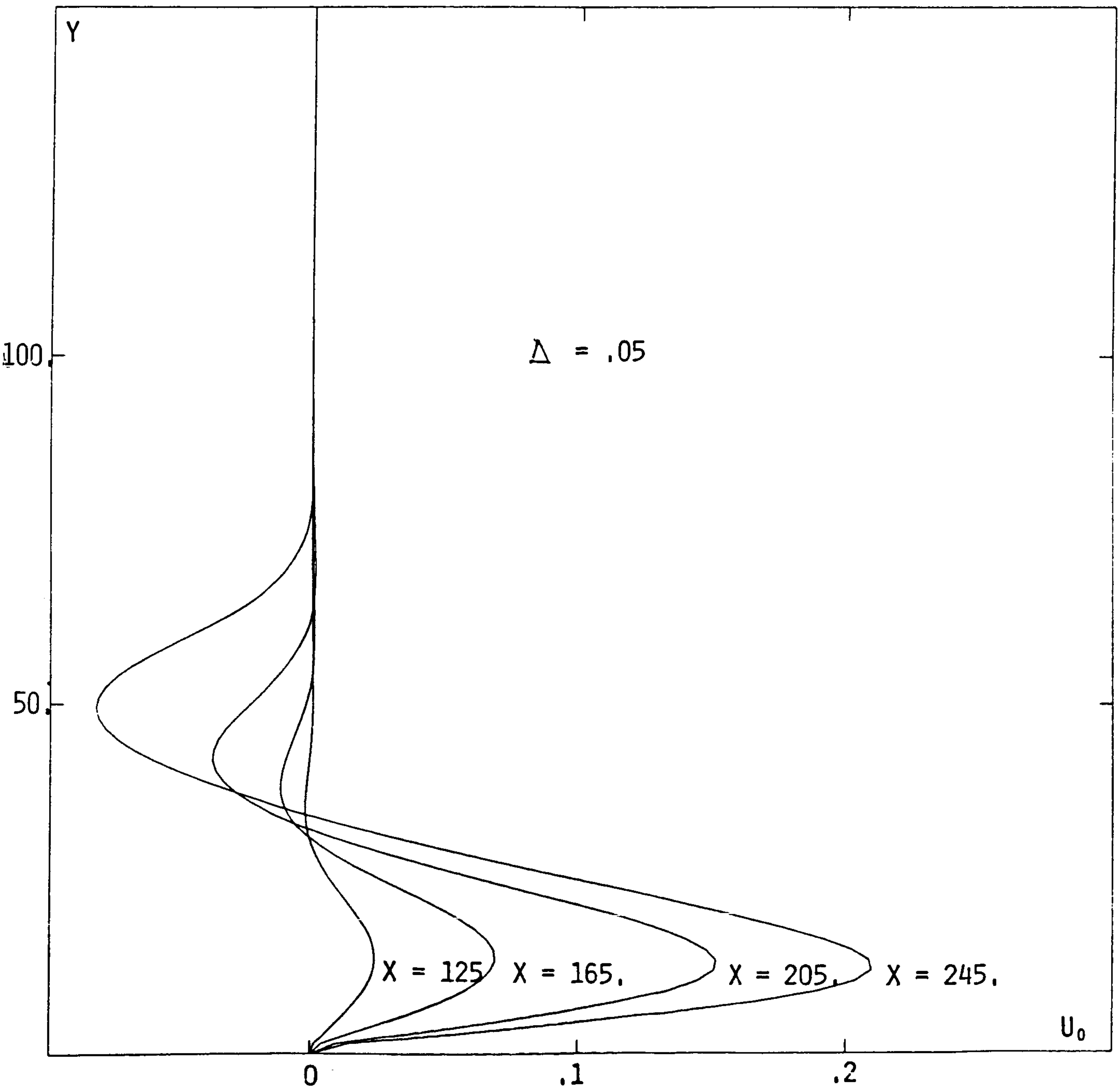

Figure 7f

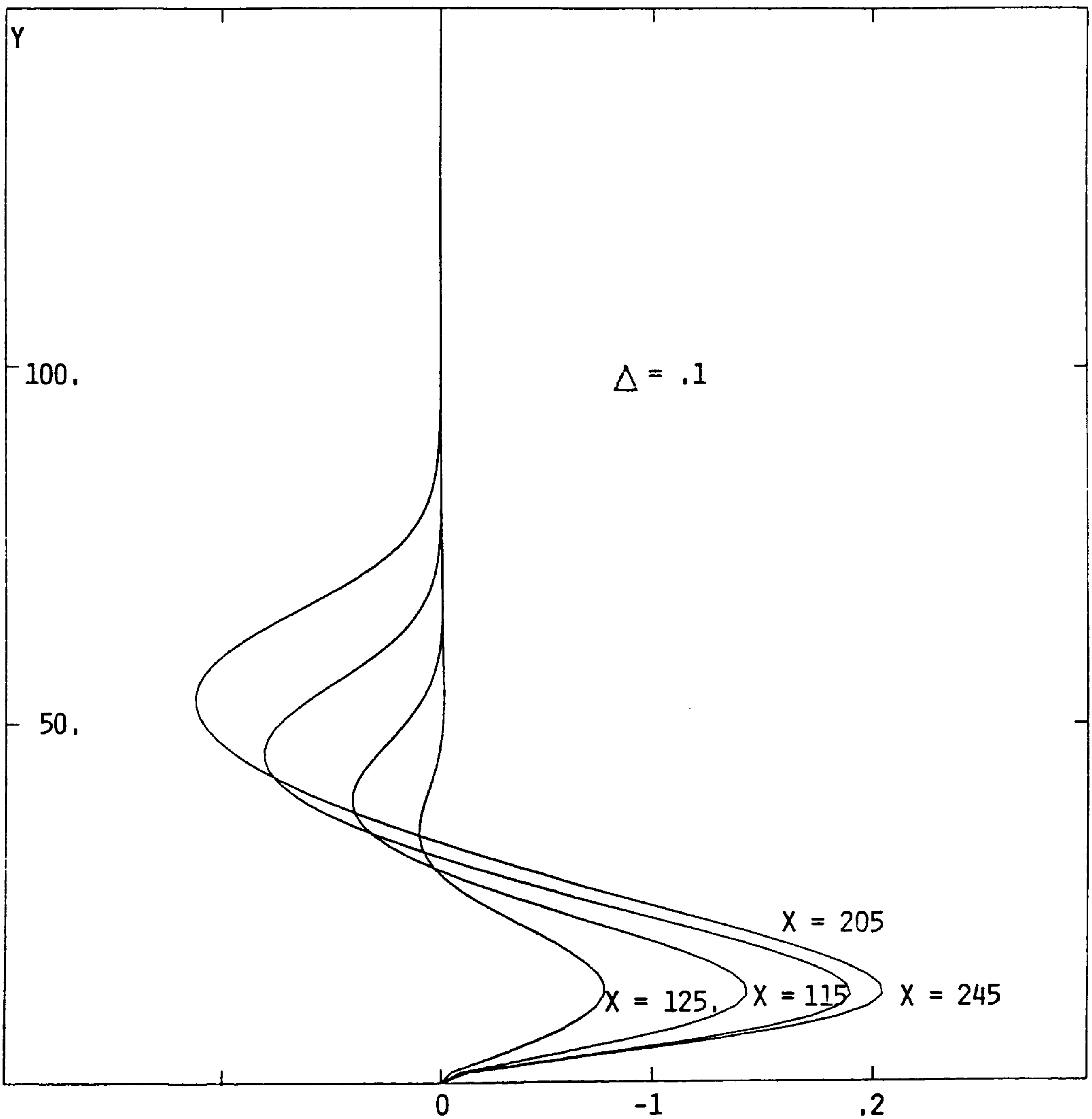

Figure 7g

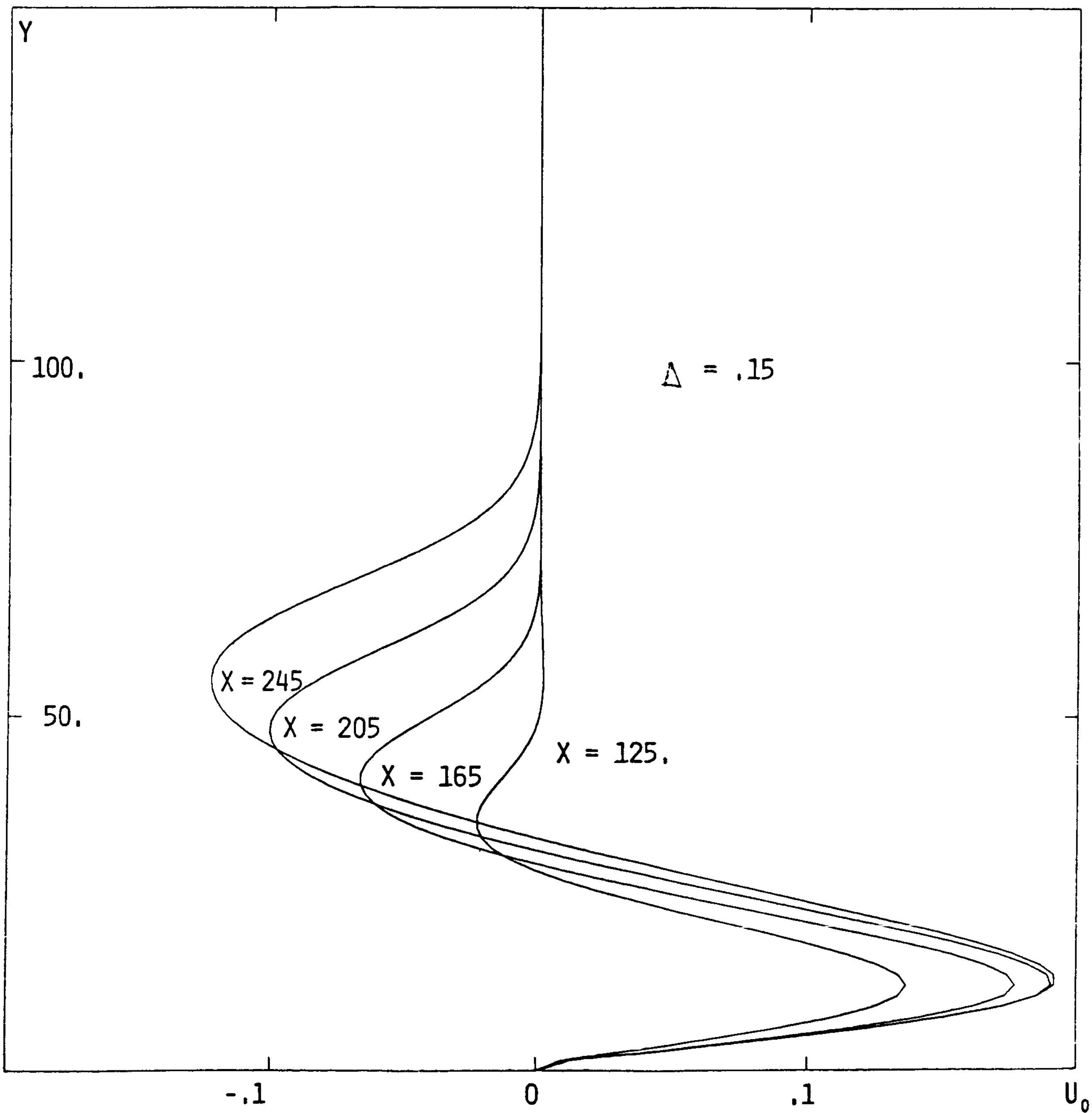

Figure 7h

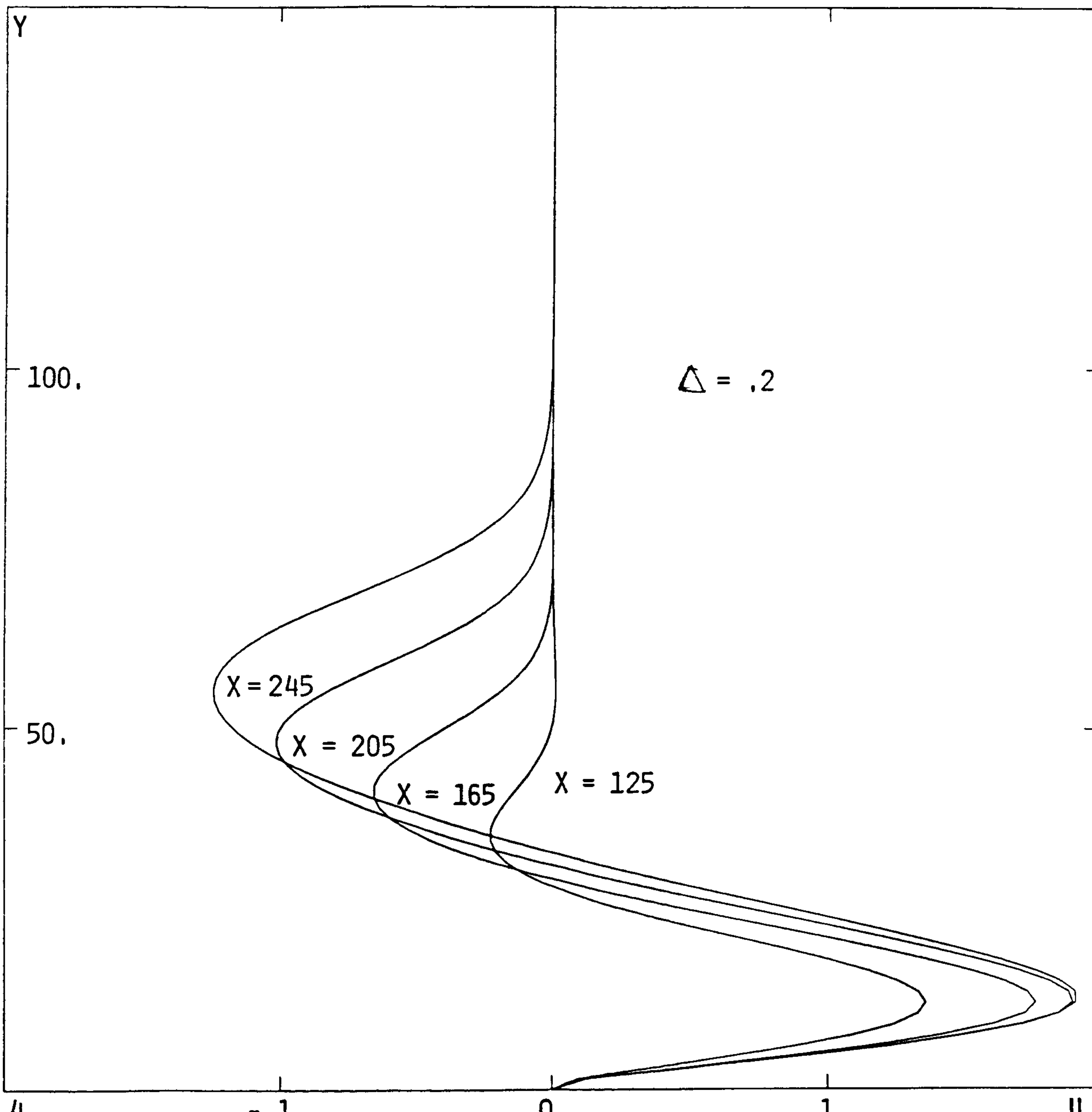

Figure 8a

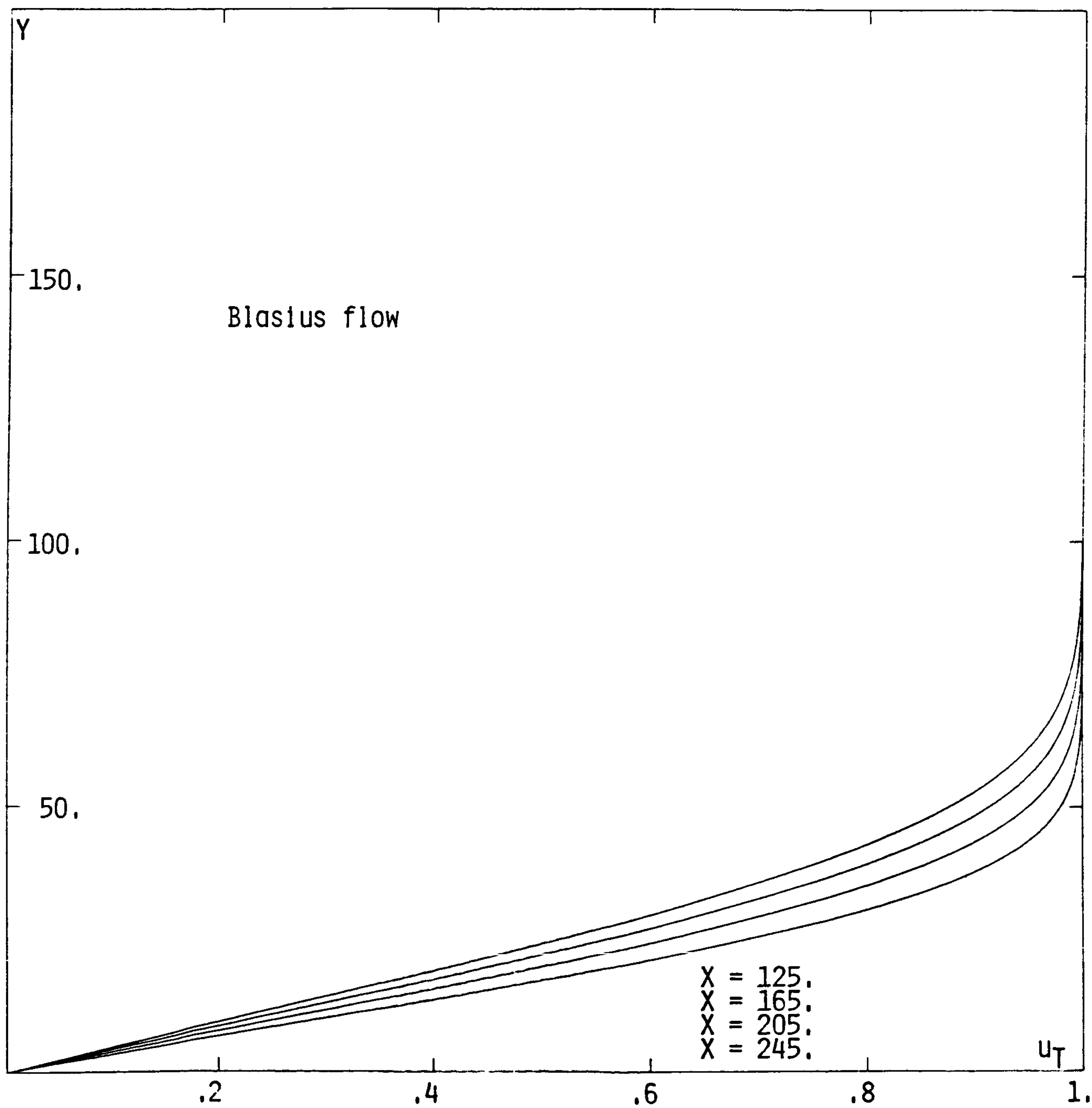

Figure 8b

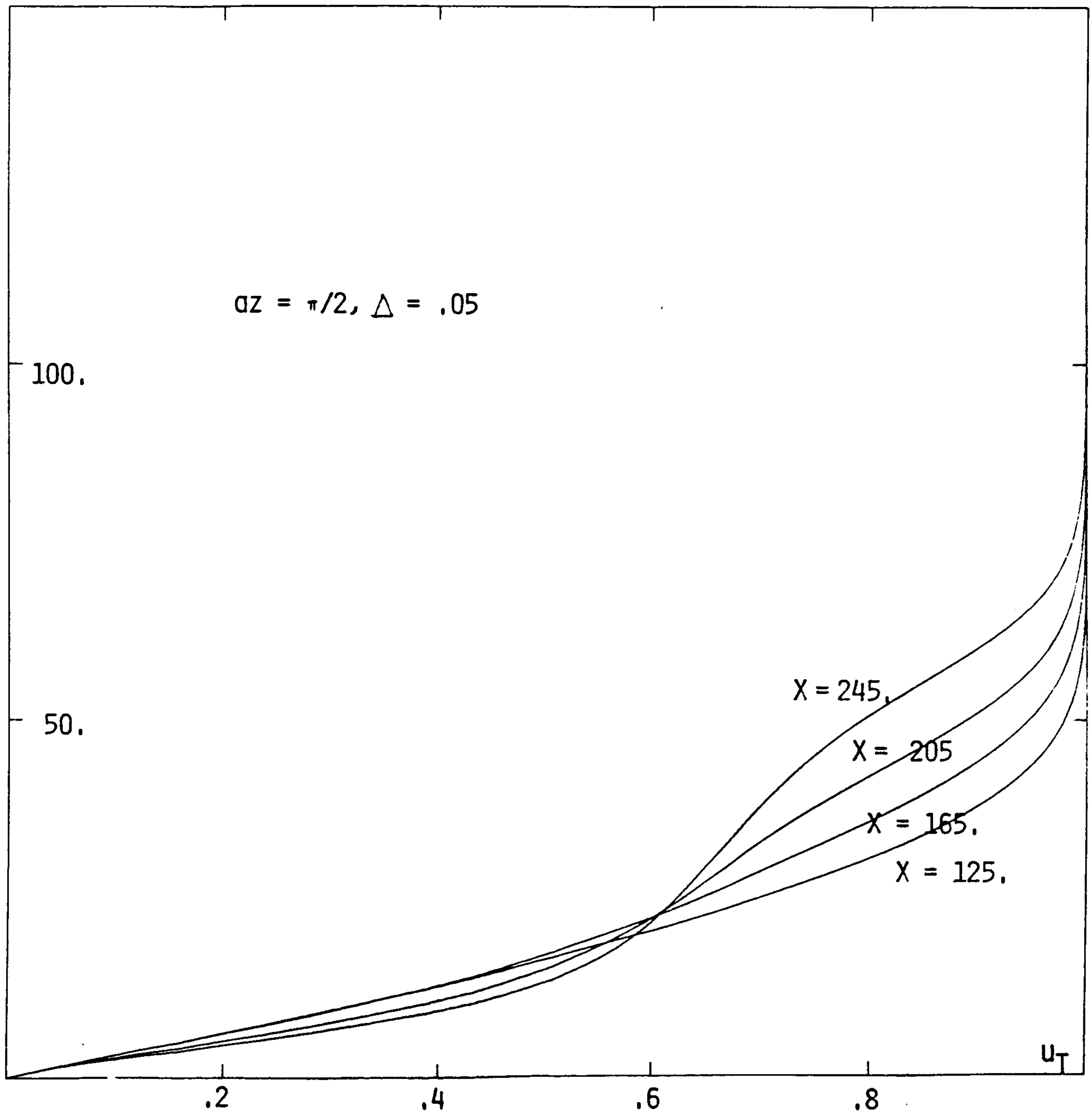

Figure 8c

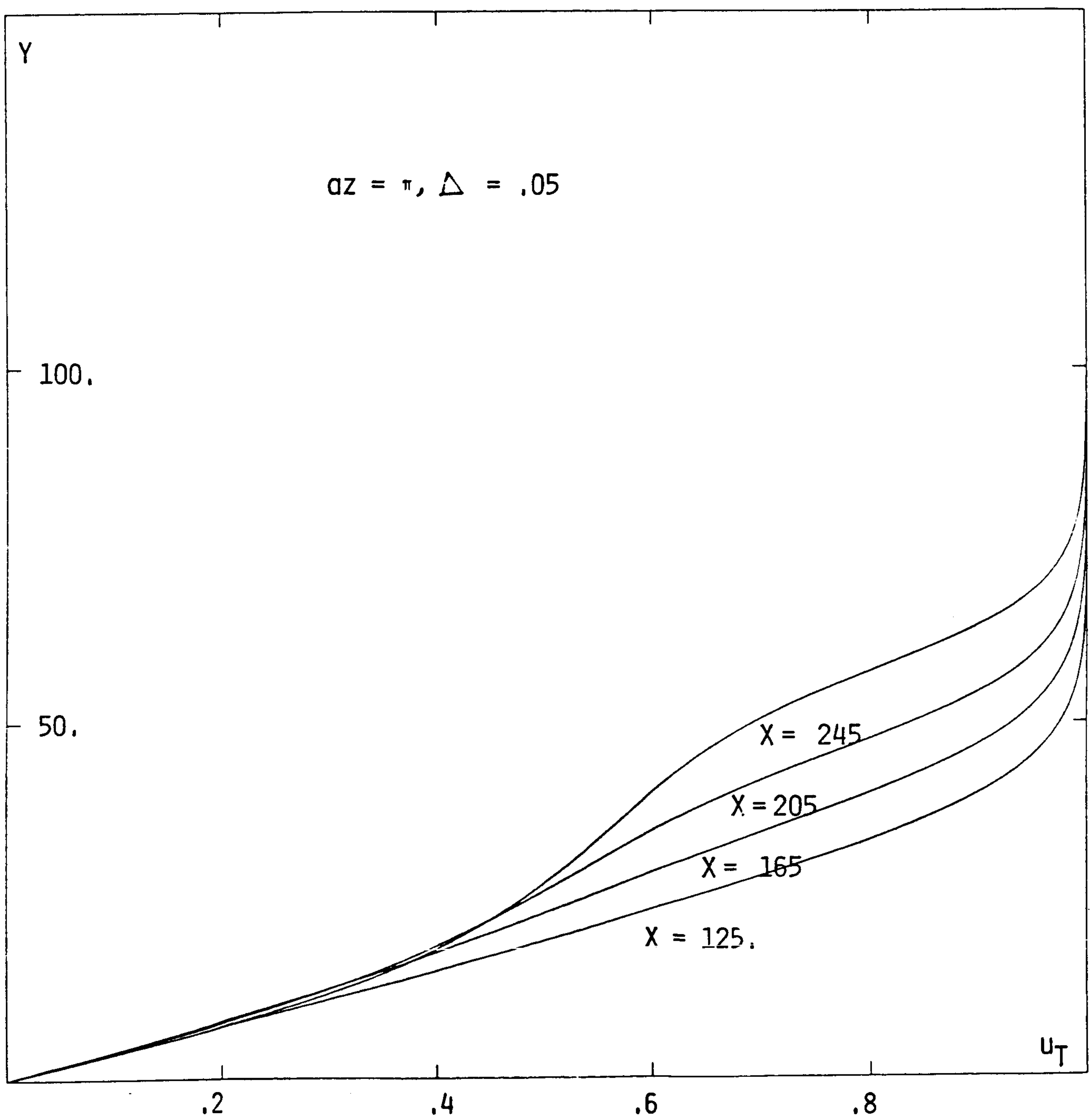

Figure 8d

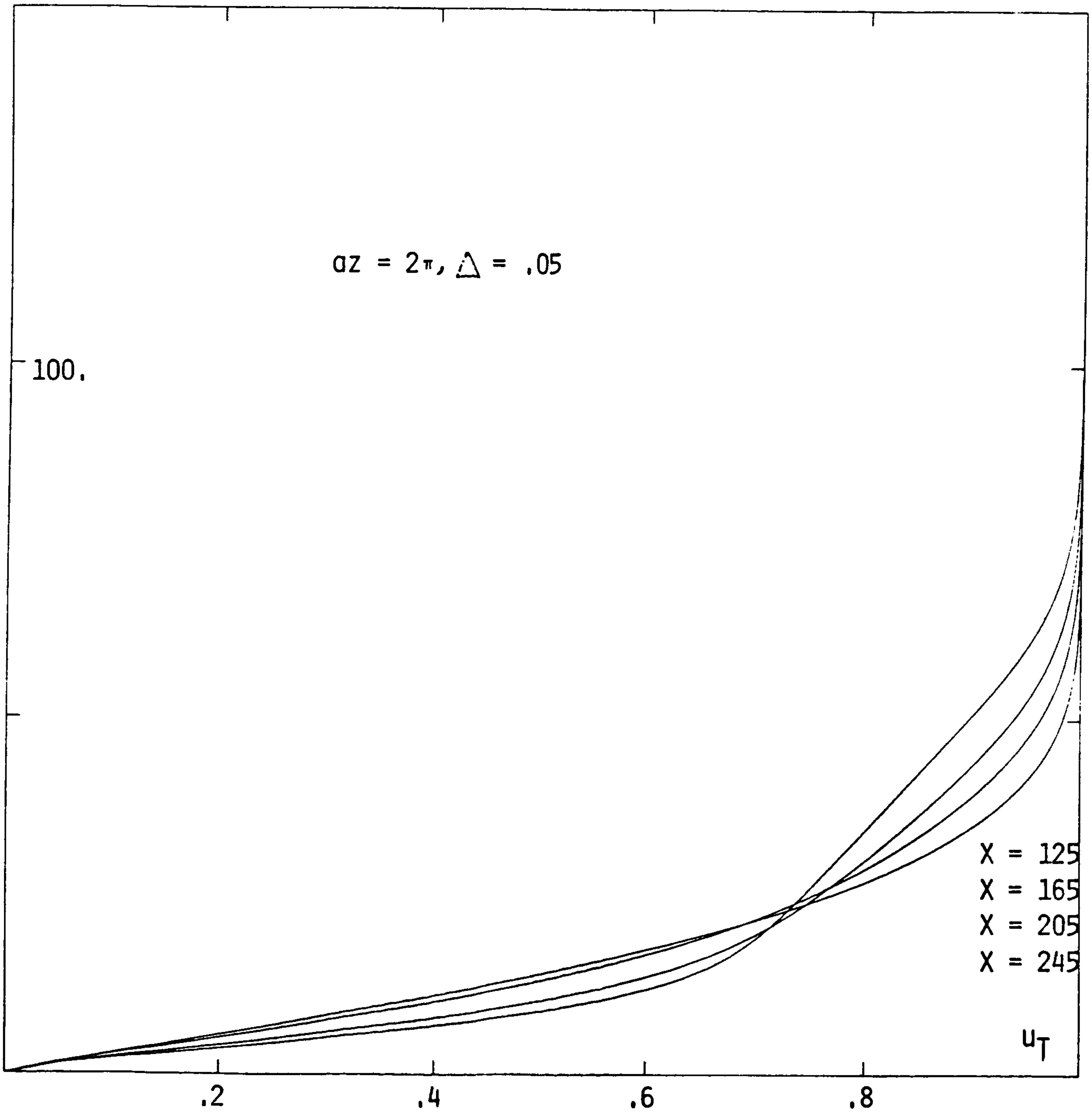

Figure 9a

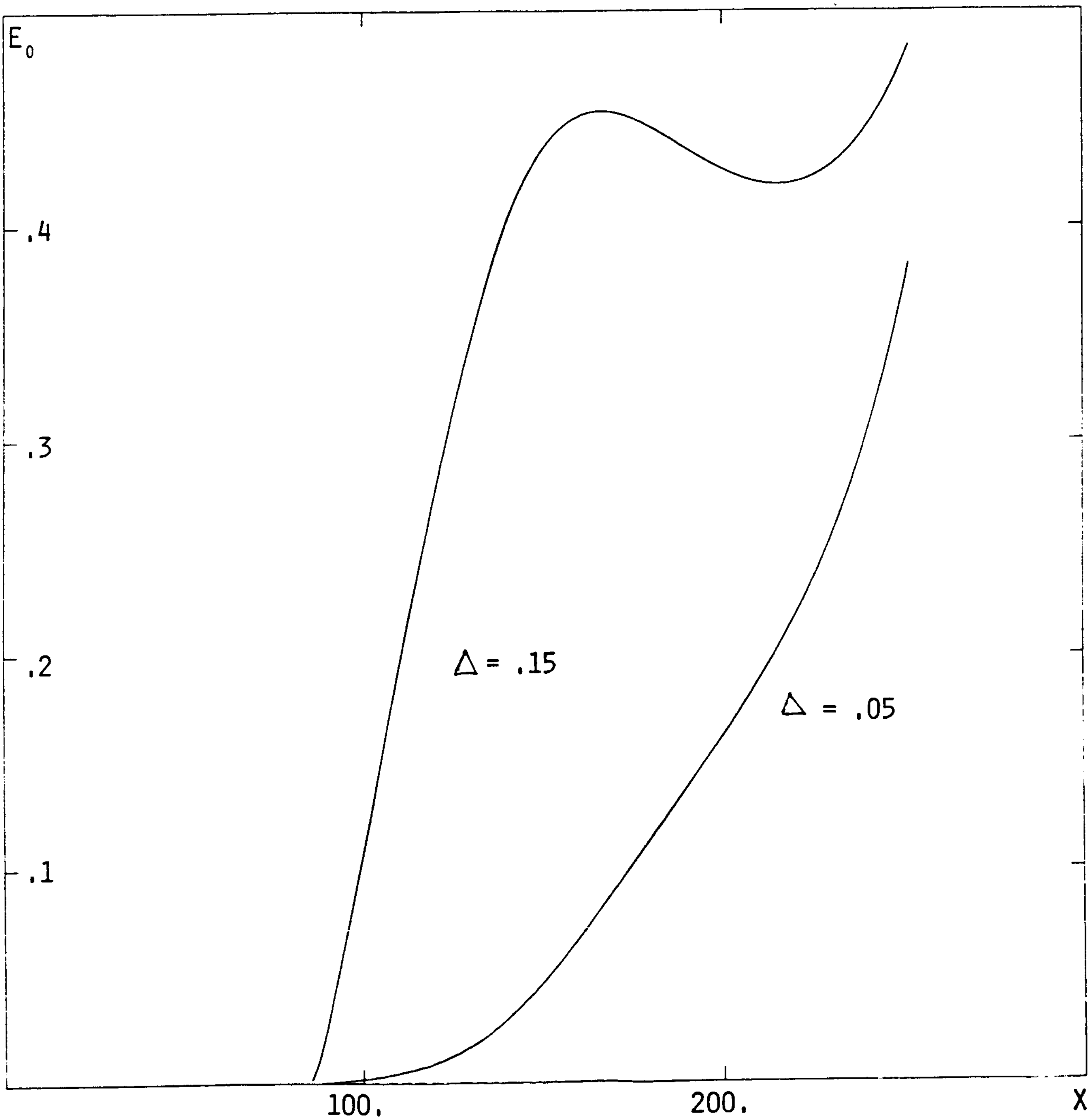

Figure 9b

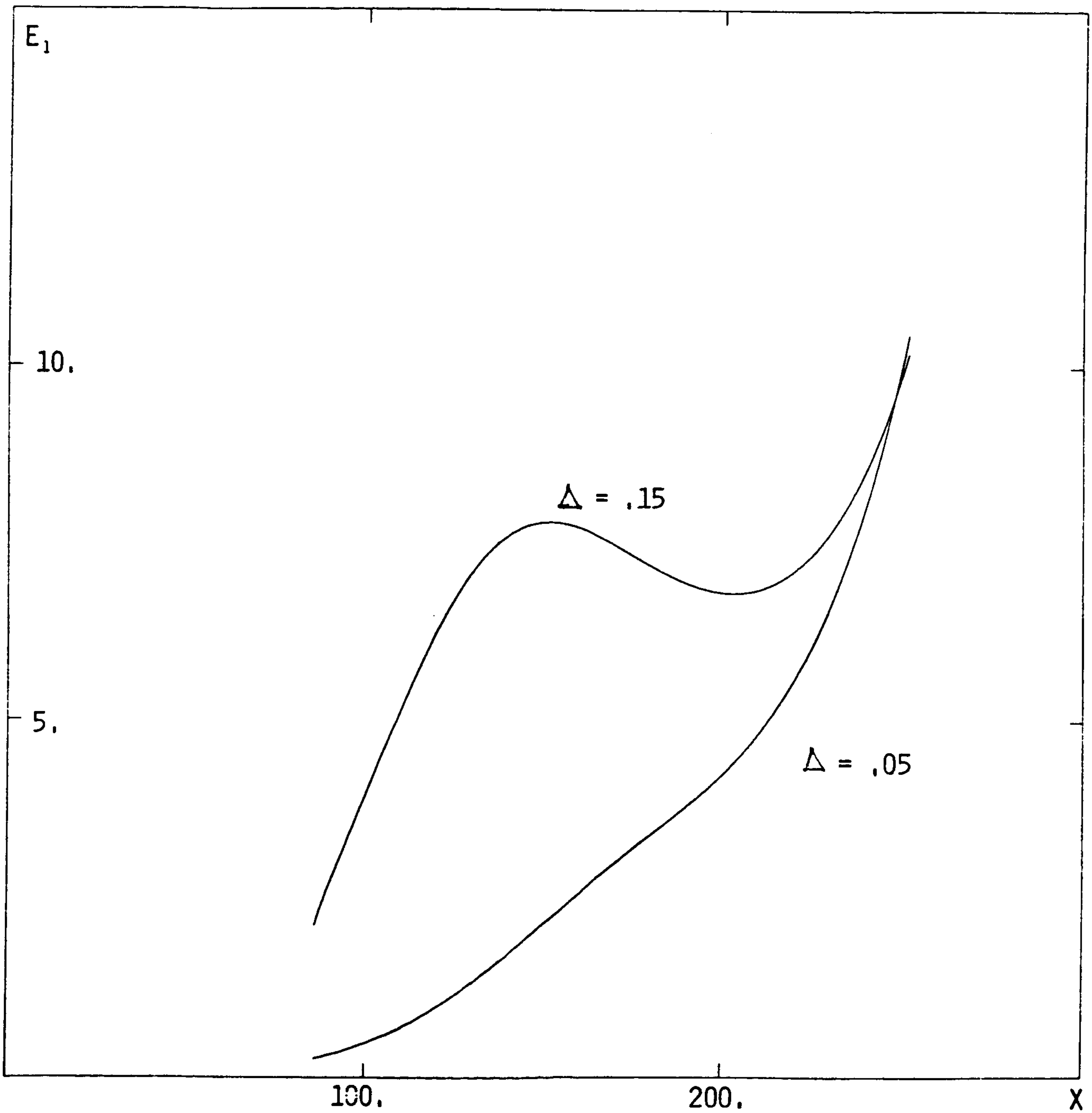

Figure 9c

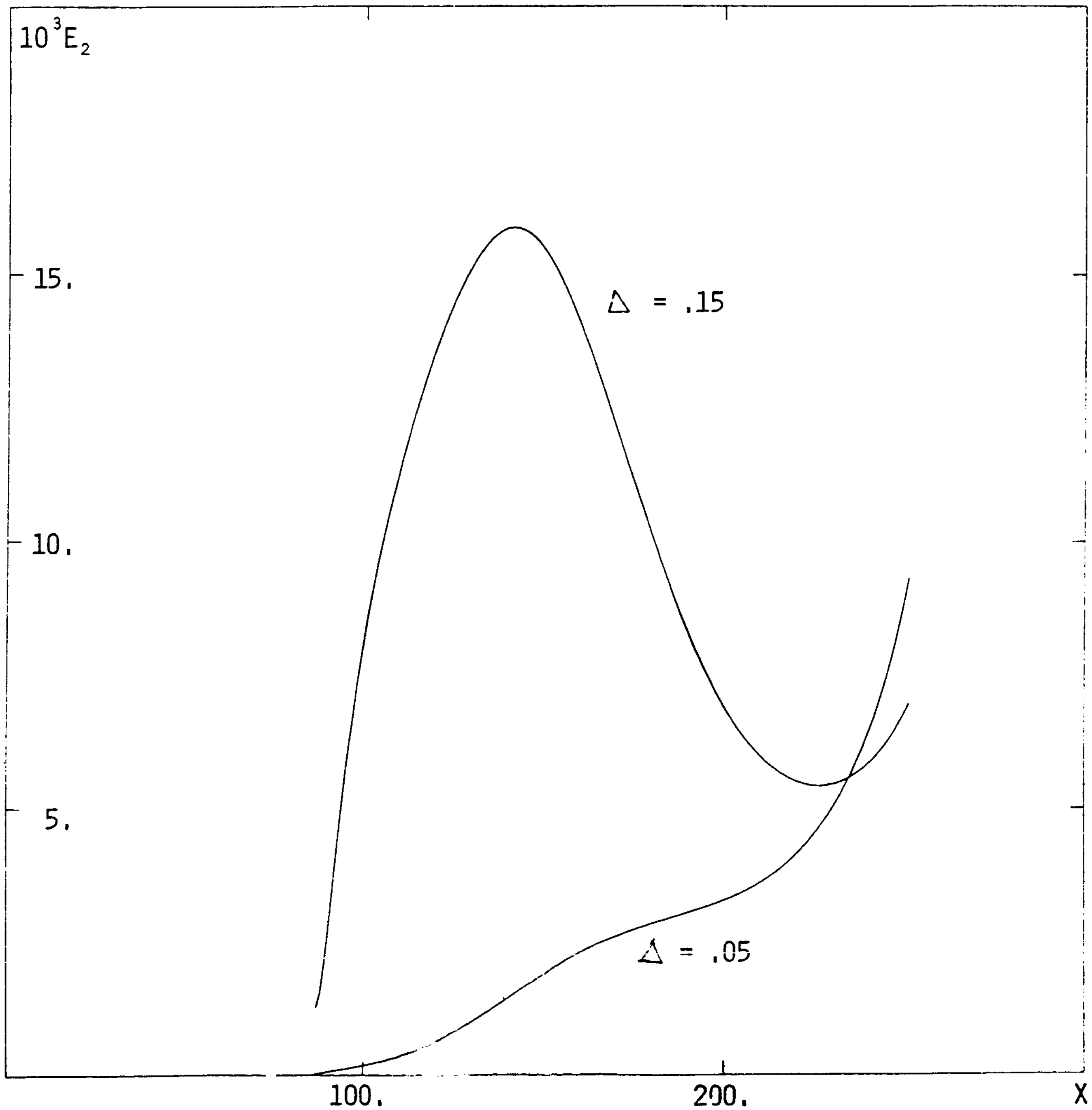

Standard Bibliographic Page

1. Report No. NASA CR-178215 ICASE Report No. 86-83	2. Government Accession No.	3. Recipient's Catalog No.
4. Title and Subtitle THE NONLINEAR DEVELOPMENT OF GORTLER VORTICES IN GROWING BOUNDARY LAYERS		5. Report Date December 1986
		6. Performing Organization Code
7. Author(s) Philip Hall		8. Performing Organization Report No. 86-83
9. Performing Organization Name and Address Institute for Computer Applications in Science and Engineering Mail Stop 132C, NASA Langley Research Center Hampton, VA 23665-5225		10. Work Unit No.
		11. Contract or Grant No. NAS1-18107
12. Sponsoring Agency Name and Address National Aeronautics and Space Administration Washington, D.C. 20546		13. Type of Report and Period Covered Contractor Report
		14. Sponsoring Agency Code 505-90-21-01

15. Supplementary Notes

Langley Technical Monitor: J. C. South

Submitted to J. Fluid Mech.

Final Report

16. Abstract

The development of Gortler vortices in boundary layers over curved walls in the nonlinear regime is investigated. The growth of the boundary layer makes a parallel flow analysis impossible except in the high wavenumber regime so in general the instability equations must be integrated numerically. Here the spanwise dependence of the basic flow is described using Fourier series expansion whilst the normal and streamwise variations are taken into account using finite differences. The calculations suggest that a given disturbance imposed at some position along the wall will eventually reach a local equilibrium state essentially independent of the initial conditions. In fact, the equilibrium state reached is qualitatively similar to the large amplitude high wave-number solution described asymptotically by Hall (1982b). In general, it is found that the nonlinear interactions are dominated by a 'mean field' type of interaction between the mean flow and the fundamental. Thus, even though higher harmonics of the fundamental are necessarily generated, most of the disturbance energy is confined to the mean flow correction and the fundamental. A major result of our calculations is the finding that the downstream velocity field develops a strongly inflectional character as the flow moves downstream. The latter result suggests that the major effect of Gortler vortices on boundary layers of practical importance might be to make them highly receptive to rapidly growing Rayleigh modes of instability.

17. Key Words (Suggested by Authors(s)) Gortler vortices, boundary layers		18. Distribution Statement 34 - Fluid Mechanics Unclassified - unlimited	
19. Security Classif.(of this report) Unclassified	20. Security Classif.(of this page) Unclassified	21. No. of Pages 52	22. Price A04